Applied Soft Computing 113 (2021) 107940

Contents lists available at ScienceDirect

Applied Soft Computing

journal homepage: www.elsevier.com/locate/asoc

System for adaptive extraction of non-invasive fetal electrocardiogram

Katerina Barnova [a], Radek Martinek [a], Rene Jaros [a], Radana Kahankova [a,*], Khosrow Behbehani [b], Vaclav Snasel [c]

[a] Department of Cybernetics and Biomedical Engineering, Faculty of Electrical Engineering and Computer Science, VSB–Technical University of Ostrava, 708 00, Ostrava-Poruba, Czechia
[b] Department of Bioengineering, University of Texas at Arlington, Arlington, TX, USA
[c] Department of Computer Science, Faculty of Electrical Engineering and Computer Science, VSB–Technical University of Ostrava, Ostrava-Poruba, Czechia

ARTICLE INFO

Article history:
Received 3 May 2021
Received in revised form 19 August 2021
Accepted 22 September 2021
Available online 8 October 2021

Keywords:
Adaptive filtration
Complete ensemble empirical mode decomposition with adaptive noise (CEEMDAN)
Extraction algorithms
Fast transversal filter (FTF)
Fetal electrocardiography
Fetal heart rate (fHR)
Hybrid system
Independent component analysis (ICA)
Non-invasive fetal monitoring

ABSTRACT

This study aimed to find the most suitable combination of adaptive and non-adaptive methods for extraction of non-invasive fetal electrocardiogram (NI-fECG) using signals recorded from the mother's abdomen. Among the nine methods considered, the combination of independent component analysis (ICA), fast transversal filter (FTF), and complementary ensemble empirical mode decomposition with adaptive noise (CEEMDAN) proved to be the most effective for the extraction of fECG from abdominal recordings. This combined method was suitable due to both being effective in extracting fECG and being less computationally complex. Further, so far, FTF and CEEMDAN methods have not been extensively tested for fECG extraction, and in particular, have not been examined as a hybrid method. The ICA-FTF-CEEMDAN hybrid algorithm was tested on two patient databases: Fetal Electrocardiograms, Direct and Abdominal with Reference Heartbeats Annotations (FECGDARHA) and PhysioNet Challenge 2013. The evaluation of the accuracy of fQRS complexes detection was performed using the following parameters: accuracy (ACC), sensitivity (SE), positive predictive value (PPV), and F1 score. The fetal heart rate (fHR) determination accuracy was evaluated using Bland–Altman plots and fHR traces. When testing on the FECGDARHA database, average values of ACC = 92.98%, SE = 95.33%, PPV = 96.4% and F1 = 95.86% for detection fQRS were achieved. The error in estimating the fHR was -1.02 ± 7.02 ($\mu \pm 1.96\sigma$) bpm. When testing on the Challenge 2013 database, average values of ACC = 78.47%, SE = 82.06%, PPV = 87.90% and F1 = 84.62% for fQRS detection were achieved, and the error in estimating the fHR was -6.62 ± 10.33 ($\mu \pm 1.96\sigma$) bpm. In addition, a non-invasive morphological analysis (ST analysis) was performed on the records from the FECGDARHA database, which was accurate in 7 of 12 records with values of $\mu < 0.03$ and values of $\pm 1.96\sigma < 0.04$.

1. Introduction

Fetal hypoxia is one of the most common causes of perinatal morbidity and mortality [1,2]. Fetal hypoxia is a condition that develops over the course of pregnancy. In the initial stage (hypoxemia), there is a decrease in oxygen saturation in the arterial blood, but cellular and organ functions are not affected. When hypoxemia worsens, the fetal's adaptive and compensatory mechanisms are triggered, allowing them to survive in this state for several days/weeks without any significant harm [3]. If the oxygen saturation of fetal blood is further reduced, its deficiency begins to manifest itself in peripheral tissues, and the anaerobic mechanism is triggered resulting in hypoxia. The fetus may remain in this condition for several hours without permanent damage [1,4]. However, a condition that requires an immediate resolution in a matter of minutes is asphyxia. Blood oxygen saturation is extremely low, and anaerobic metabolism takes place not only in peripheral tissues but also in the heart and brain, followed by systemic collapse with heart and central nervous system failure [5].

Accurate and timely diagnosis of hypoxia is, therefore, a primary goal in fetal monitoring. The first efforts to monitor the fetus were based on intermittent auscultation of fetal heart sounds and calculation of fetal heart rate (fHR) [6]. Thanks to advances in science and technology, the first monitors based on phonocardiography monitoring heart sounds were invented in the second half of the 20th century. These devices were not able to distinguish between the maternal and fetal heart sounds, so the automatic determination of fHR was not possible [7]. A major breakthrough came with the invention of cardiotocography (CTG), which is based on fetal monitoring using simultaneous

* Corresponding author.
E-mail address: radana.kahankova@vsb.cz (R. Kahankova).

https://doi.org/10.1016/j.asoc.2021.107940

recording of fHR and uterine contractions [8]. By introducing this non-invasive method in the 1960s and enabling continuous monitoring in clinical practice [9], there was a significant reduction in fetal deaths. Unfortunately, CTG proved to suffer from a high rate of false positives (up to 60%) [10–12], and the detection of hypoxia based only on the assessment of fHR turned out to not be accurate enough [10,13]. This led to a high number of unnecessarily performed caesarean sections, which are a great burden with added risks for both the mother and the fetus [13–15]. More accurate fetal monitoring was enabled by Neoventa Medical (Molndal, Sweden) devices; this company was the first to introduce the innovative STAN S31 ST segment analyzer into the clinical practice in 2007 [9]. This device records the fetal electrocardiogram (fECG) by attaching a bipolar spiral electrode on the fetal scalp (i.e., fetal scalp electrode, FSE) and analyzing the changes in the morphology of the fECG signal; in particular the T/QRS ratio (known as ST analysis, STAN) [16,17]. Therefore, simultaneous fHR and STAN monitoring help to increase the accuracy of detecting fetal hypoxia, hence reducing the number of unnecessary caesarean sections [18]. Invasiveness of the method entails the risk of infection when placing the scalp electrode on the fetus and the serious limitation that it can be implemented only after the rupture of the amniotic fluid membrane during childbirth method of monitoring fECG less desirable [19,20].

For these reasons, attention has recently been focused on the development of non-invasive versions of fECG. This method is based on recording the electrical activity of the fetal heart using electrodes that are placed on the mother's abdomen. The possibility of recording fECG during pregnancy and childbirth, non-invasiveness and greater safety of the method are significant advantages of this method [21]. Nevertheless, when using this technique to record fetal cardiac activity, maternal cardiac activity is mixed with the recorded signal with a significantly larger magnitude than the fECG magnitude. Moreover, the maternal and fetal components overlap in both the time and frequency domains, so extracting a good quality fECG continues to be a challenging task [19,21].

The benefit of our proposed hybrid method enabling it to achieve high quality extraction is that it combines the advantages of three techniques: independent component analysis (ICA), fast transversal filter (FTF) and complementary ensemble empirical mode decomposition with adaptive noise (CEEMDAN). The advantage of the ICA method is that it requires solely abdominal signals (aECG) at the input, from which it is able to estimate the maternal ECG (mECG) and the aECG signal with enhanced fetal component. Therefore, there is no need to use another chest lead to record the mECG signal. In clinical practice, mECG signal recorded from mother's chest is often of a poor quality and the measurement itself is uncomfortable since it decreases her mobility. Therefore, using the mECG and aECG signals estimated by means of the ICA method leads to better extraction with FTF algorithm, which is prone to poor quality input signals. The adaptive FTF algorithm excels in eliminating mECG almost completely since it is able to adapt to the nature of the signal on its input. The CEEMDAN method can smooth the residue of the mECG component in the resulting fECG signal without distorting its morphology, as is the case with other smoothing methods, such as the wavelet transform (WT) [22].

Thus, the use of solely aECG signals, quality extraction of fECG using adaptive filtering, and smoothing the resulting fECG signal, while remaining its morphology and thus allowing ST segment analysis, is the main benefit of this algorithm. In addition, the results of the study showed that with the help of well-scanned non-invasive signals, it is possible to obtain the same accurate results of fHR and ST analysis as in the case of the invasive variant. Another benefit is its high computing speed, which would allow its implementation in real-time operating devices.

2. State of the art

There are numerous filtration methods that can be applied to extract useful information from the non-invasive fECG recording. These are, for example, methods based on the blind source separation (BSS) technique [23–25], which can extract original source signals from a signal mixture. This group of methods also include the popular ICA [26–28] and the principal component analysis (PCA) [26,29]. Another important method for fECG extraction is the application of WT [30–32] or the template subtraction method (TS), which is based on subtracting the template (parent component) from the abdominal signals [33,34]. More advanced methods include the application of artificial neural networks (ANNs) [35,36] that are able to learn and analyze complex data. In this category, the adaptive linear network (ADALINE) [37,38], which is a single-layer artificial neural network that uses linear activation functions to update its weights, is also worth mentioning.

Recent studies, [39–45], have demonstrated that hybrid systems that combine several algorithms are more effective in extracting accurate fECG compared with using only a single algorithm. We have previously presented such methods. For instance, in [22] two hybrid methods combining ICA, recursive least squares (RLS) and WT (i.e., ICA-RLS-WT) as well as a combination of ICA, adaptive neuro-fuzzy interference system (ANFIS) and WT (i.e., ICA-ANFIS-WT) were presented. In [46], we presented procedures based on combining empirical mode decomposition (EMD) with some of the other methods that resulted in ICA-EMD, ICA-EMD-WT and ICA-RLS-EMD. The best results were obtained with ICA-RLS-EMD method, but for some recordings, the extraction was not efficient enough. The aim of this study was to find suitable alternatives to RLS and EMD methods that will help in to achieving more accurate extraction. These assumptions were met by the FTF and CEEMDAN methods and therefore they were selected for implementation and testing. A comparison of the main advantages and limitations of the individual fECG extraction methods that have been used in the past for fECG extraction are summarized in Table 1.

2.1. Adaptive filters

Adaptive filters are very popular and frequently used as signal processing tools nowadays. These filters are characterized by the ability to automatically adjust the adaptive coefficients of the filter. This occurs by minimizing the error signal, which is defined as the difference between the desired output and the actual output of the system [47,48]. An adaptive system usually consists of two parts, a digital filter, and an adaptive algorithm for adjusting the filter coefficients [49]. Currently, there is a large number of types of adaptive filters, an overview of which is summarized in [50]. Adaptive filters can generally be divided into two groups, based on the approach they use to optimize the error function. These are the stochastic gradient adaptation methods and the optimal recursive adaptation methods [47,50]. The stochastic gradient adaptation group includes the least mean square (LMS) method, which, due to its simplicity and low computational complexity, is one of the most widely used techniques. The step size parameter determines the convergence rate and it also affects how fast and how close the adaptive filter approaches the desired output values [51,52]. The normalized LMS (NLMS) algorithm was created by modifying the standard LMS algorithm; it excels due to its simplicity and robust performance.

The optimal recursive adaptation methods can include the RLS algorithm, the advantage of which is excellent performance, when working in time-varying environments, and fast convergence. There are some disadvantages for these methods in the

Table 1
Comparison of advantages and disadvantages of different fECG extraction algorithms.

Method	Advantages	Limitations
ICA, PCA	Stable	To achieve greater accuracy of algorithms, it is necessary to use a larger number of quality input signals
WT	Fast	Distortion of signal morphology
TS	Simple	mQRS detection accuracy significantly influences the overall performance
ANNs, ANFIS, ADALINE	Precise	The performance of the algorithm depends on the correct setting of a large number of parameters
RLS	Precise	As the filter order increases, the computational speed decreases
FTF	Fast	The performance of the algorithm strongly depends on the quality of the input signals
EMD	Stable	The extraction efficacy may be adversely affected by *mode mixing*
CEEMDAN	Stable	As the number of ensemble trials increases, the computational speed decreases

form of increased computational complexity [53]. This group can also include a FTF, which was designed specially to reduce the computational complexity of the RLS filter while maintaining the speed of convergence. Its concept is structurally based on four different filters working simultaneously on one task [54–56].

For the purposes of extracting fECG, the LMS, NLMS, DLMS, BLMS filters were implemented and compared in the past in [48]. The best results were achieved using the BLMS filter, and on the other hand, the worst results were obtained using the NLMS filter. The efficacy of LMS a NLMS methods was also compared in [35], however, in this case, no significant differences were found between these filter performances. The authors of the study [57] tested NLMS and RLS filters to extract fECG. It has been proven that better results were obtained using the RLS algorithm, and, in addition, it converged faster than the NLMS algorithm. The RLS filter outperformed also the LMS algorithm in [58] according to the evaluation based on the sensitivity (SE), positive predictive value (PPV) and F1 metrics. The LMS algorithm was effective in combination with the ICA [41], the WT [32,59,60], or with LMS and ANN [61]. An interesting approach is also combining multiple adaptive filters, as proposed in [62]. The best results were achieved using a combination of LMS and RLS algorithms.

2.2. Empirical mode decomposition based methods

The EMD method was proposed in [63] for addressing nonlinear and non-stationary issues. Its principle is based on the decomposition of the input complex signal into simpler signals, which are called intrinsic mode functions (IMFs). By summing all IMFs, the original signal can be reconstructed [63–65]. The advantage of EMD lies in its high speed compared to other versions of this method. Its disadvantage, on the other hand, lies in the limitation called *mode mixing* which affects the resulting extraction quality [64]. This problem is due to the fact that one of the IMFs contains several components with different frequencies, or components with similar frequencies are contained in several different IMFs [66]. To address this shortcoming, the ensemble empirical mode decomposition (EEMD) method was proposed in [67]. This is based on the principle of adding independent Gaussian white noise to the input signal and performing several ensemble trials. Each trial uses the same procedure as EMD. The resulting IMFs are obtained by averaging the corresponding IMFs from all ensemble trials [64,68]. By applying the EEMD method, the risk of *mode mixing* occurrence can be eliminated, but a new problem arose when reconstructing the original signal. This reconstructed signal contained significant residues of Gaussian white noise [64,69]. To prevent this while preserving the benefits of the EEMD method, the complementary ensemble empirical mode decomposition (CEEMD) was designed in [69]. The principle of CEEMD is the same as EEMD, but instead of fully independent Gaussian white noise, complementary paired positive and negative white noise is generated, which leads to mutual elimination of noise residues in the resulting signal [64,69]. The low computational speed of the algorithms, which decreases with the increasing number of ensemble trials, is another disadvantage of the EEMD method, as well as CEEMD [64]. For this reason, in [70], CEEMDAN, which uses a smaller number of iterations (i.e., nearly a half), thus increasing the computational efficiency of the algorithm, was proposed [70].

For fECG extraction, the EMD method was successfully tested in combination with ICA in [71] or in combination with multiple signal classification [72]. In [40], the authors concluded that the system combining the EEMD, ICA, and wavelet shrinkage showed to be most effective in suppressing maternal component compared to the system combining EMD and wavelet shrinkage. The performance of the EMD, EEMD and CEEMD methods was compared for fECG extraction in combination with correlation analysis in [73]. The CEEMD method provided better frequency resolution of IMFs than EMD or EEMD and more accurate reconstruction of the original signal. An accurate fECG extraction was also achieved using CEEMDAN in [74]. According to [75], the EMD and EEMD methods were outperformed by the CEEMDAN algorithm, since it could provide better frequency separation of the extracted IMFs.

A comparison of the basic representatives of adaptive filters and EMD-based methods is summarized in Table 2. The evaluation of individual parameters was achieved as follows:

1. *Performance:* the performance was evaluated using the high, medium, and low categories in terms of the accuracy of fHR determination of the extracted signals.
   (a) *High:* the method was able to filter out all disturbances highly effectively and, in the statistical evaluation of fHR, values $\leq$ 95% were achieved using the ACC, SE, PPV and F1 parameters.
   (b) *Medium:* the method was able to filter out most interference, but some interference residues led to ACC, SE, PPV and F1 parameter values $\leq$ 80% in the statistical evaluation of fHR.
   (c) *Low:* the method was not able to sufficiently eliminate the interference and, in the statistical evaluation of fHR, values $<$ 80% were achieved using the ACC, SE, PPV and F1 parameters.
2. *Computational complexity:* the parameter was assigned three levels of high, medium, and low categories, based on subjective evaluation.
   (a) *High:* reflects a computationally complex method that cannot be used in real-time applications.

Table 2
Performance parameters of basic adaptive filters and EMD-based methods.

Algorithm		Performance	Computational complexity	References
Adaptive methods	LMS	Medium	Low	Wu et al. [32], Camps et al. [35], Martinek et al. [47], Kaur et al. [51], Shengkui [52], Swarnalatha et al. [62], Gupta et al. [41], Behar et al. [58], Lima-Herrera et al. [59], Ziani et al. [60], Kaleem et al. [61]
	NLMS	Medium	Low	Camps et al. [35], Martinek et al. [48], Kaur et al. [51], Swarnalatha et al. [62], Liu et al. [57]
	RLS	High	Medium	Martinek et al. [47], Diniz [53], Swarnalatha et al. [62], Behar et al. [58], Liu et al. [57]
	FTF	High	Low	Cioffi et al. [54], Setareh et al. [55], Bessekri et al. [56]
EMD-based methods	EMD	Low	Low	Huang et al. [63], Ren et al. [64], Gao et al. [66], Liu et al. [76], Azbari et al. [73], Taralunga et al. [71], Wei et al. [72]
	EEMD	Medium	High	Ren et al. [64], Wu et al. [67], Chang [68], Liu et al. [76], Azbari et al. [73], Liu et al. [40]
	CEEMD	Medium	High	Ren et al. [64], Yeh et al. [69], Liu et al. [76], Azbari et al. [73]
	CEEMDAN	Medium	Medium	Ren et al. [64], Torres et al. [70], Colominas et al. [77], Liu et al. [76], Li et al. [78], Queyam et al. [75], Muduli et al. [74]

(b) *Medium:* denotes a slightly more computationally demanding method that can be used in real-time applications after optimization.
(c) *Low:* assigned to a computationally not complex method that can be used in real-time applications.

3. Materials and methods

This section describes the methods implemented within the hybrid system. Based on the literature search and study of the issue, ICA, FTF, and CEEMDAN were selected. Furthermore, the proposed hybrid system, its optimal settings, the parameters used to evaluate the performance of the hybrid system and the database used for testing each method are described.

3.1. Independent component analysis

The ICA extraction technique belongs to the group of blind source separation methods. Its principle is based on the decomposition of the input mixed signal into the original separate source components [26,79–81]. In the case of fECG extraction, the input mixed signal represents the aECG signal recorded from the mother's abdominal wall, and the source components consist of fECG, mECG and noise. To perform the extraction correctly, the assumptions that the source components are non-Gaussian signals and are statistically independent of each other must be met [79,82]. More accurate source signals extraction can be achieved using a larger number of input signals. In the past, several extended versions of the ICA method were presented: the computationally efficient FastICA algorithm [83], efficient version of the FastICA (EFICA) [84] or joint approximate diagonalization of eigen-matrices (JADE) [28]. In this study, the FastICA version using a fixed-point iteration scheme was applied to obtain results faster than the classical version. More detailed information on the ICA method can be obtained in [26–28,79,82].

3.2. Fast transversal filter

The goal of the adaptive FTF filter is to minimize the error signal between the desired and actual output by automatically adjusting the adaptive coefficients. The FTF filter achieves the same performance as the RLS, but it possesses a much higher computational speed. The FTF filter is not burdened by a linear increase in the computation time with increasing filter order, as is the case with RLS [55,85]. Therefore, its use is a very suitable solution for real-time applications. The principle of the filter is based on the use of four transversal filters working simultaneously on one task.

These four transversal filters designed to compute update quantities as described in [55,86] include:

- *Forward prediction transversal filter* – this block calculates the forward filter weights in such way that minimizes the least-square error of the subsequent sample based on the previous ones. To calculate the error of estimation for the forward prediction, the filter uses *a priori* and a posterior filter weights as well as the minimum weighted least squares error.
- *Backward prediction transversal filter* – calculates the backward filter weights in such way that minimizes the least-square error of the $n - M$th sample using the vector input $\mathbf{x}_b(n) = [x(n)x(n-1)x(n-2)\ldots x(n-M+1)]^T$. As with forward prediction, this filter calculates the minimum weighted least squares error and the posterior and *prior* filter weights.
- *Gain computation transversal filter* – is used for recursive computation of the gain vector. The gain vector is used to update the forward, backward, and joint-process estimation filter weights. It also provides recursive computation of the conversion factor [55].
- *Joint-process estimation transversal filter* – determines the filter weight so that the error between the desired and actual signal is as small as possible. Thus, this block calculates filter

weights in the same way as the adaptive algorithms used earlier.

The disadvantage of the algorithm is the instability after a finite number of iterations. However, several approaches [85,87] have been proposed to solve this problem. Usually, these approaches are based on expressing the update equations in different forms [86]. The detailed description of this filter is very extensive, and a complete description of the algorithm can be obtained in [54–56,85,86].

3.3. Complementary ensemble empirical mode decomposition with adaptive noise

The principle of the CEEMDAN method is based on the decomposition of a more complex input signal into simpler signals, called IMFs [70,88]. The method builds upon the previously presented EEMD method [67], which in turn is built upon EMD procedures [63]. The main idea is to add independent Gaussian white noise to the input signal and perform several ensemble trials. The resulting IMFs are obtained by averaging the corresponding IMFs from all ensemble trials [64,68]. The CEEMDAN method differs in the following aspect: the addition of paired positive and negative adaptive white noise to the input signal, which better eliminates the *mode mixing* issue, and, also, the resulting IMFs are calculated sequentially. That is, each IMF is used to calculate the succeeding IMF [76,77]. This results in a smaller number of iterations which leads to an increase in the computational speed of the algorithm [70].

The algorithm can be summarized as follows:

- First, the number of ensemble trials realizations N and the standard deviation of the added noise series N_{std} are set.
- Gaussian noise $w(t)$ with unit variance is added to the original signal $x(t)$.

$$s(t) = x(t) + \beta_0 w(t), \tag{1}$$

  where β_0 is the level of noise.
- Signal $s(t)$ is decomposed N-times using the EMD method and the first $IMF_1(t)$ is obtained by averaging all $IMF_1(t)$ related to N trials. The EMD method is based on identifying local minima and maxima in the signal $s(t)$ followed by detecting the upper and lower envelopes of the signal using a cubic spline by combining all maxima and minima, respectively. The mean of the envelopes is then subtracted from the original signal $x(t)$ and $IMF_1(t)$ is obtained as follows:

$$IMF_1(t) = x(t) - \langle M(s(t))\rangle, \tag{2}$$

  where $\langle M(s(t))\rangle$ represents the mean of the envelopes of the signal $s(t)$.
- The residual signal $r_1(t)$ is calculated by subtracting the first extracted $IMF_1(t)$ from the original signal $x(t)$.

$$r_1(t) = x(t) - IMF_1(t). \tag{3}$$

- The second $IMF_2(t)$ is extracted in the same manner as the first one, but instead of the original signal $x(t)$, the residual signal $r_1(t)$ is used.

$$IMF_2(t) = r_1(t) - \langle M(r_1(t) + \beta_1 w(t))\rangle. \tag{4}$$

- To obtain additional IMFs, the entire procedure is repeated, but $r_k(t)$ is used as the further residual after the kth decomposition, where $k = 1, 2, \ldots, K$. The $IMF_k(t)$ is obtained as:

$$IMF_k(t) = r_{k-1}(t) - \langle M(r_{k-1}(t) + \beta_{k-1} w(t))\rangle. \tag{5}$$

- The whole procedure is repeated until the residual signal cannot be extracted (i.e. the residual signal is a monotone function, a function with only one extremum or a constant).

The motivation to use ICA, FTF and CEEMDAN methods in fECG extraction system and post-processing was following:

1. Fetal ECG extraction – accurate fECG extraction is a very challenging task in which conventional techniques are not efficient enough. Adaptive algorithms (especially RLS) have proven to be very promising for fECG extraction in our previous research [22,46]. The RLS algorithm was able to extract fECG with high accuracy, but with increasing filter order, its computational speed decreased significantly, which would make it impossible to use it in real-time applications. Therefore, an alternative was sought that could extract fECG with the same (or higher) accuracy, but much faster, even with higher filter orders. The FTF algorithm met these requirements and was selected and tested for these reasons. The FTF algorithm requires two input signals: the aECG (mixture of mECG, fECG and other interferences) and the reference mECG signal, which is modified by the FTF method so that it corresponds as closely as possible to the maternal component in the aECG signal and can be subtracted from it, thus obtaining fECG and some residual noise. In general, there are two approaches to obtain these two inputs (mECG and aECG):
   - The first involves simultaneous scanning of mECG from the mother's thorax and aECG from the abdominal area. However, the thoracic mECG signal differs from the maternal component sensed on the abdominal wall in terms of its magnitude, phase, and morphology. Moreover, in clinical practice it is quite challenging to ensure a high quality thoracic mECG signal, i.e. without artifacts that are caused by maternal movement or improper electrode placement and fixation. The quality of the extraction by an adaptive algorithm is closely connected to the quality of the input signals, and therefore distortion the maternal reference signal leads to inaccurate fECG extraction. Additionally, its measurement can be unnecessarily uncomfortable and stressful for the mother [9].
   - For these reasons, we chose the second approach, which is based on obtaining the mECG and aECG input signals solely from aECG signals. This involves implementation of a separation algorithm (such as ICA), which is able to estimate mECG and aECG with an enhanced fetal component.
2. Post-processing – for post-processing, it was necessary to select a method that would be able to remove mECG residues so that the fHR determination is accurate and at the same time would not affect the morphology of the resulting fECG waveform, so that the ST signal analysis could be performed. Past research [22] has shown that WT-based methods are not suitable for further morphological analysis, and therefore EMD-based algorithms have been considered. Among them, CEEMDAN, which was used in the hybrid system for the final smoothing of fECG, proved to be the most suitable in terms of the efficacy and computational complexity.

The advantages of individual methods and their combination to achieve accurate and time-efficient fECG extraction can be summarized as follows:

- ICA-FastICA is a computationally efficient method with low memory requirements [89] but is not able to sufficiently suppress mECG and extract fECG in sufficient quality when used on its own. On the other hand, using solely aECG input signals, it can provide a good estimate of the mECG and aECG signal with enhanced fetal component that are used as inputs for FTF algorithm.
- FTF-adaptive filters generally excel in performance and adaptability in time-varying environments (which is also the case with fECG) [53]. In case that the filter receives high-quality input signals (aECG and mECG), it is able to extract an accurate fECG signal only with minor mECG residue. Moreover, it performs in a time-efficient manner even with increasing filter order.
- CEEMDAN method proved to be the best compromise between performance and computational complexity among other EMD-based algorithms. Despite the fact that it cannot extract fECG or mECG on its own, it has proven to be suitable for use in the post-processing phase for the additional suppression of mECG residues. In addition, it did not significantly alter the morphology of the fECG signal, allowing accurate morphological analysis to be performed.

3.4. Dataset

In this work, the hybrid algorithm was tested on two databases. The first one is called the *Fetal Electrocardiograms, Direct and Abdominal with Reference Heartbeats Annotations* (FECG-DARHA) and is freely available in *figshare repository* [90]. The dataset contains 12 five-minute recordings obtained from women between the 38th and 42nd week of gestation. The recordings were obtained at an advanced stage of child development. Each recording contains four abdominal signals recorded from the mother's abdominal area using standard Ag/AgCl electrodes. At the same time, the direct fECG signal was recorded from the fetal head using a sterile spiral electrode. The signals were recorded using the KOMPOREL system and digitized with 16-bit resolution and a sampling frequency of 1000 Hz for the direct fECG and 500 Hz for the abdominal signals. In addition, this system automatically detected and marked the positions of fetal R-peaks, the accuracy of which was verified by clinical experts. The dataset, therefore, also includes annotations providing the exact positions of fetal R-peaks. Data collection was performed at the Department of Obstetrics and Gynaecology of the Medical University of Silesia in Katowice, Poland [90].

The second database is called the *Physionet Challenge 2013* [91]. The database was created as part of the *PhysioNet Computing in Cardiology Challenge 2013*, which aimed to support the development of algorithms for accurate localization of fQRS complexes and fQT interval estimation in non-invasive fECG signals. Each recording contains four abdominal signals one minute long and with a sampling frequency of 1000 Hz. At the same time, direct fECG signals were also captured using a fetal scalp electrode, which served to create reference annotations indicating the position of fQRS complexes. Nevertheless, only annotations are part of the database; direct fECG signals are not part of the database. The data were obtained from different women with a different gestational age of the fetus. Different devices with different resolutions and configurations were used to record the signal [91].

3.5. Hybrid system design

This section describes the ICA-FTF-CEEMDAN hybrid system for the extraction of non-invasive fECG, including the parameters that were used to evaluate the quality of the extraction. The hybrid system can be described using the following steps:

- *Selection of suitable aECG signals:* first, it was necessary to select at least two input signals, as this is a multi-channel algorithm. Four input signals were available for each recording, but not all of them were captured well (e.g. the fetal component acquired very low magnitudes). Therefore, only the most suitable signals were selected so as not to unnecessarily reduce the extraction effectiveness.
- *Preprocessing:* input aECG signals were preprocessed using a bandpass finite impulse response filter (BPF FIR) with a frequency range of 3–150 Hz (fQRS complexes occur in the range of 10–15 Hz [20]) and a filter order of 500 Hz. The filter was used to remove isoline fluctuations and motion artifacts, see Fig. 1.
- *FastICA:* Furthermore, the ICA method, which is based on the decomposition of a mixture of signals into the original source components, was applied. In this case, a very effective FastICA algorithm was used; it was arbitrarily set to 20 iterations and decomposition of the input aECG signals into three components. The first component corresponded to aECG with highlighted fECG (referred to as $aECG_{ICA}$), the second mECG (referred to as $mECG_{ICA}$) and the third one corresponded to noise, see Fig. 2. As the polarity of the ICA components was rotated during the extraction, an algorithm checking the highest positive and negative amplitude within 50 ms from the detected R-peaks was used, and, based on this, the algorithm determined whether the signal was rotated correctly or whether it needed to be rotated.
- *FTF:* the first two components of $aECG_{ICA}$ and $mECG_{ICA}$ were time and amplitude aligned, using automatic centering. The centering was based on detecting the positions and amplitudes of maternal R-peaks. The shifts between the individual maternal R-peaks in $aECG_{ICA}$ and the maternal R-peaks in $mECG_{ICA}$ were determined and the average time shift was calculated. The signals were aligned by this average time shift. Similarly, differences between amplitudes were determined. The signal with the higher average amplitude of the maternal R-peaks was proportionally reduced relative to the signal with lower average amplitude. Such centered signals were used as inputs of the adaptive FTF algorithm. The $aECG_{ICA}$ component was used as the primary input (desired signal). And, the $mECG_{ICA}$ component, which the FTF algorithm filtered into the approximate form of the mECG component contained in the primary input, was used as the second input. Subsequently, the $mECG_{FTF}$ component extracted by the FTF filter was subtracted from the $aECG_{ICA}$ signal, thus obtaining $fECG_{FTF}$ with a suppressed maternal component, see Fig. 3. As for the FTF algorithm, forgetting factor λ was set to a value of 1 due to optimization, and filter order M was tested in the range of 1 to 100 with increments of 1.
- *CEEMDAN:* since the $fECG_{FTF}$ signal contained residual noise, the CEEMDAN method was used to remove it. It decomposed the input $fECG_{FTF}$ signal to simpler signals, so-called IMFs. The decomposition into IMFs continued until the stopping condition was reached (the residual signal was a monotone function, a function with only one extremum or a constant). A total of 10 IMFs were extracted, and a final signal indicated as $fECG_{CEEMDAN}$ was generated by selecting the appropriate IMFs, see Fig. 4. For this method, it was necessary to set the value of the standard deviation of the added noise series N_{std} and the number of ensemble trials N. Parameter N_{std} was tested in the range of 0.1 to 0.9 in 0.1 increments. Parameter N was tested for values of 10, 30 and 60; testing for higher values was not necessary, as the extraction effectiveness was no longer improved.

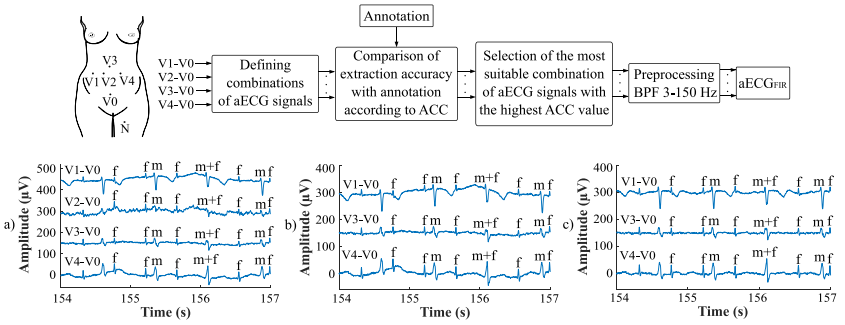

Fig. 1. Selection of suitable aECG signals and their preprocessing. Example of (a) all input aECG signals for recording r01, (b) selected aECG signals that are suitable for further processing, (c) filtering of suitable aECG signals using a BPF FIR filter in the range of 3–150 Hz.

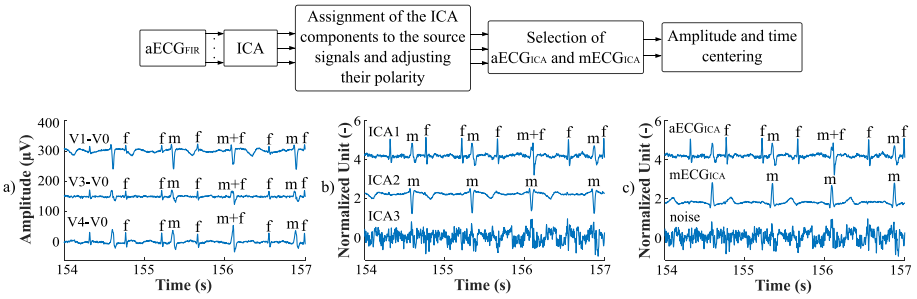

Fig. 2. Signal processing using the FastICA algorithm. Example (a) presents preprocessed input aECG signals, example (b) shows the extraction of three ICA components and example (c) represents the assignment of the ICA components to the source signals and adjusting their polarity.

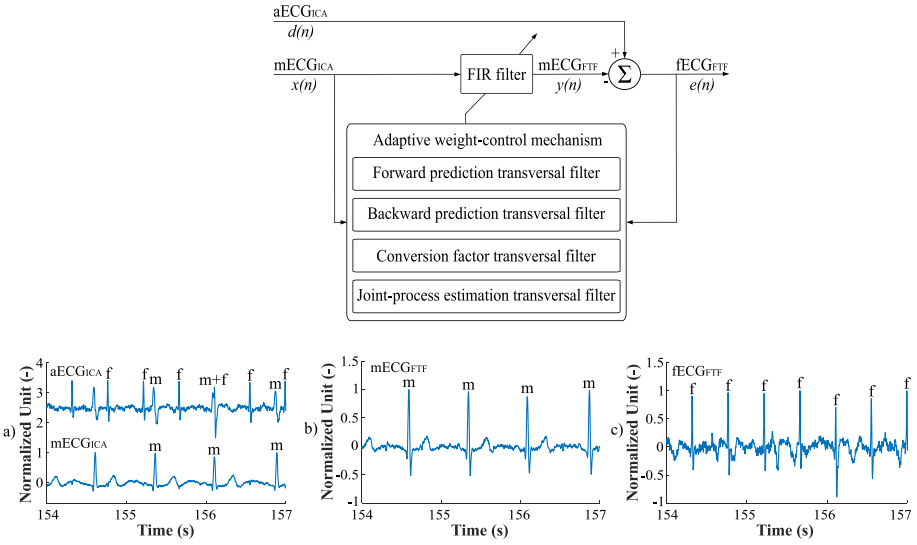

Fig. 3. Signal processing using the FTF algorithm. Example (a) presents $aECG_{ICA}$, which was used as the desired signal, indicated as $d(n)$, and $mECG_{ICA}$, which needed to be filtered by the FTF filter, indicated as $x(n)$. Example (b) shows the $mECG_{FTF}$ component that was extracted by the FTF filter, indicated as $y(n)$. The extracted $mECG_{FTF}$ was subtracted from $aECG_{ICA}$, thus creating the $fECG_{FTF}$ error signal, indicated as $e(n)$. Example (c) represents the $fECG_{FTF}$ output signal.

- *Algorithms settings:* to achieve the most efficient extraction of fECG, optimal setting of the parameters of the individual algorithms was crucial. Selection of suitable input aECG signals, parameter M and forgetting factor λ setting for the FTF filter, N, N_{std} parameters of the CEEMDAN method and selection of suitable IMFs by means of which the resulting $fECG_{CEEMDAN}$ was generated. This was achieved using an automated algorithm that compared various combinations of the parameters set and selected the combination that provided fECG signal with the highest accuracy according to the ACC value. Accuracy comparison was carried out using annotations. The most suitable parameters values for the individual recordings are summarized for the FECGDARHA database and the Challenge database in Tables 3 and 4, respectively.
- *Evaluation parameters:* the effectiveness of the hybrid method was evaluated, both in terms of the accuracy of fetal R-peaks detection and in terms of the accuracy of fHR determination. First, fetal R-peaks were detected using a detector based on continuous wavelet transform (CWT). The positions of the detected R-peak positions were compared with the reference R-peak positions given in the annotations. If the position of the detected R-peak was ±50 ms from the reference position, it was marked as true positive

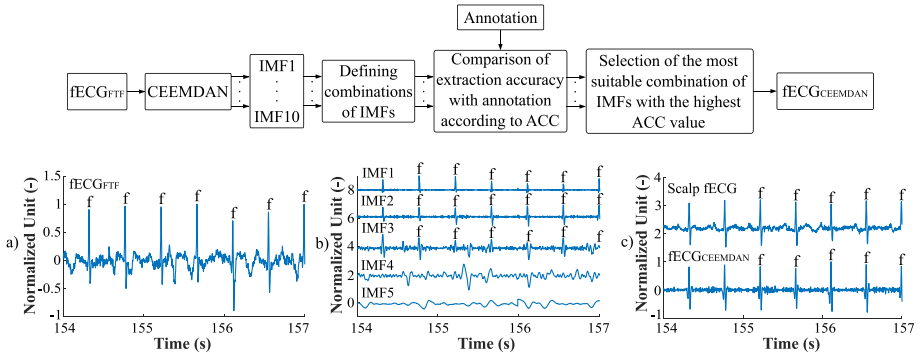

Fig. 4. Signal processing using the CEEMDAN algorithm. Example (a) presents the input fECG signal processed by the FTF algorithm, example (b) shows the first 5 extracted IMFs, example (c) shows the resulting extracted $fECG_{CEEMDAN}$ signal using a hybrid algorithm compared to the reference recording which was made using a scalp electrode.

Table 3
ICA-FTF-CEEMDAN algorithm settings for recordings from the FECGDARHA database.

Recordings	Combination of electrodes	ICA	FTF		CEEMDAN		
		Number of iterations	M	λ	N	N_{std}	IMFs
r01	1, 3, 4	20	2	1	10	0.2	2+3
r02	1, 2, 3, 4	20	99	1	10	0.6	3+4
r03	2, 4	20	90	1	60	0.7	3
r04	1, 4	20	38	1	30	0.9	2+5
r05	1, 4	20	21	1	10	0.5	2+3+7
r06	1, 2, 3, 4	20	16	1	30	0.5	3+4
r07	1, 4	20	36	1	30	0.9	2+5
r08	1, 4	20	2	1	60	0.4	4
r09	1, 2, 4	20	16	1	10	0.6	2+3+4+6
r10	1, 2, 3, 4	20	54	1	60	0.4	2+4+6
r11	1, 2, 3, 4	20	100	1	60	0.7	3
r12	1, 2, 3, 4	20	16	1	30	0.3	2+3+6+7

Table 4
ICA-FTF-CEEMDAN algorithm settings for recordings from the Challenge database.

Recordings	Combination of electrodes	ICA	FTF		CEEMDAN		
		Number of iterations	M	λ	N	N_{std}	IMFs
a01	1, 3, 4	20	11	1	10	0.8	2+3+5+7
a02	1, 2, 4	20	2	1	60	0.5	4+6+8
a03	1, 4	20	68	1	10	0.5	3+6+8
a04	1, 2	20	30	1	10	0.5	2+3
a05	1,3	20	30	1	10	0.5	2+3
a06	2, 4	20	25	1	60	0.4	3+6+7
a07	1, 2, 3, 4	20	4	1	10	0.4	3+5+6+8
a08	1, 4	20	2	1	10	0.3	2
a09	1, 4	20	99	1	30	0.6	3
a10	2, 4	20	84	1	10	0.9	2
a11	1, 4	20	68	1	30	0.3	2+3+5
a12	1,3, 4	20	9	1	30	0.6	3+6+7
a13	2, 4	20	35	1	60	0.9	4+7
a14	1, 2, 3, 4	20	10	1	10	0.7	3+4
a15	1, 4	20	49	1	10	0.3	2
a16	1, 4	20	68	1	10	0.8	4+5
a17	1, 4	20	2	1	10	0.3	2
a18	1, 2, 3, 4	20	33	1	10	0.1	5+9
a19	3, 4	20	35	1	60	0.6	4
a20	1, 4	20	99	1	60	0.9	4+5
a21	2, 3, 4	20	87	1	30	0.9	2+3+4+5+7
a22	1, 4	20	2	1	10	0.2	2
a23	1, 3	20	47	1	30	0.9	2+4+5
a24	1, 3	20	52	1	60	0.9	3+4
a25	2, 3	20	90	1	60	0.9	4

(TP), i.e. as a correctly detected (true) R-peak. Detected R-peaks in the extracted signal, which fell outside this interval, were marked as false positive (FP), so it corresponded to the detection of a peak that was not a fetal one (for example, the maternal residue or other interference). Omitted fetal R-peaks that were in the original but were not detected by the detector were marked as false negative (FN) values (for example, the amplitude of fetal R-peaks could be suppressed by the filtration) [39,92,93]. ACC, SE, PPV and F1 indices could be determined using FN, FP, and TP values. The ACC parameter expresses how many R-peaks were detected correctly with respect to all detected and omitted R-peaks. Thus, it defines the ratio of all TP values with respect to all marked values (TP, FP, FN), see Eq. (6). The SE parameter shows how many of all existing R-peaks were correctly predicted. It is defined as the ratio of all TP values to all existing R-peaks (TP and FN), see Eq. (7). The PPV parameter tells how many of the R-peaks that were detected were *true*. Defined as the ratio of all TP values to all detected R-peaks (TP and FP), see Eq. (8). And parameter F1 takes into account both parameters SE and PPV and is defined as their harmonic average, see Eq. (9).

$$ACC = \frac{TP}{TP + FP + FN} \cdot 100\ (\%). \tag{6}$$

$$SE = \frac{TP}{TP + FN} \cdot 100\ (\%). \tag{7}$$

$$PPV = \frac{TP}{TP + FP} \cdot 100\ (\%). \tag{8}$$

$$F1 = 2 \cdot \frac{SE \cdot PPV}{SE + PPV} = \frac{2 \cdot TP}{2 \cdot TP + FP + FN} \cdot 100\ (\%). \tag{9}$$

To evaluate the fHR, it was necessary to convert the vectors of intervals between the detected positions of the R-peaks into vectors of the current fHR values. The accuracy of the fHR determination was evaluated using Bland–Altman plots, where vector of differences and vector of the average of the two signals were determined. When graphically represented, the difference is shown on the vertical axis and the average of the values is found on the horizontal axis. The middle horizontal line indicates the mean μ of all differences and, based on this line, a 95% confidence interval, which lies in the interval $\mu \pm 1.96\sigma$, is then plotted [94]. In addition, fHR traces were plotted for the comparison of fHR. To plot the fHR traces, it was necessary to create moving averages from the fHR values calculated. A width of 30 samples was the most suitable window size. A schematic representation of the procedure for evaluating the extracted signals is shown in Fig. 5.

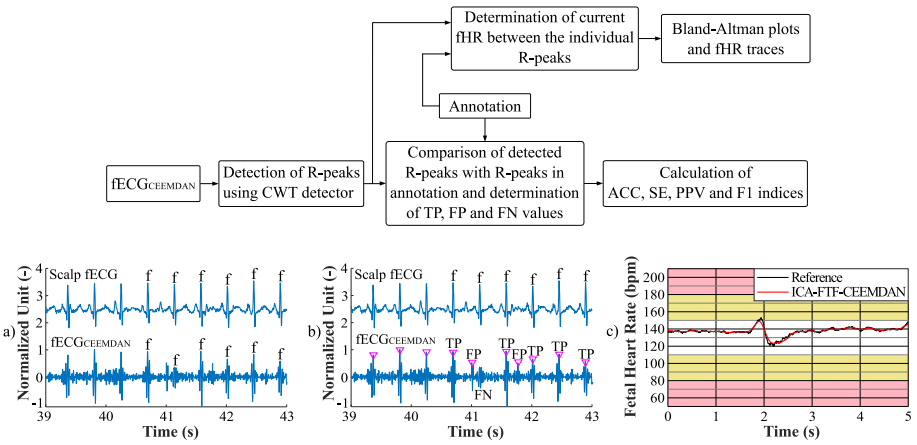

Fig. 5. Procedure for evaluation of the extracted $fECG_{CEEMDAN}$ signals. Example (a) shows the extracted $fECG_{CEEMDAN}$ signal using a hybrid algorithm in comparison with the reference recording. Example (b) demonstrates the detection of fetal R-peaks and the determination of the TP, FP, and FN values. Example (c) represents the fHR trace plotting.

- *ST segment analysis*: This method is based on monitoring the T/QRS ratio. The change in this ratio is due to a change in cellular ionic currents during anaerobic metabolism of the fetal heart. It has been shown that the combined monitoring of fHR and ST analysis leads to the early identification of cases of acidosis during childbirth, and at the same time it has been associated with reduced number of unnecessary caesarian sections [17,20]. The current disadvantage of today's ST analyzers is its invasiveness and the use being possible only during childbirth. Therefore, it is highly desirable to find a solution to perform a non-invasive ST analysis with the same accuracy as can be done invasively. In order to determine whether the determination of the ST analysis on the estimated fECG signal was accurate, it is necessary to have a reference signal measured with a scalp electrode. This is only met by the FECGDARHA database, so ST analysis was performed on 12 records from this database. Fig. 6 illustrates the ST analysis procedure which can be summarized in the following steps:

    1. Determination of the R-peak positions in the estimated fECG signal using a CWT detector. Annotations with R oscillation positions are available for the reference signal and their detection is therefore not necessary.
    2. Averaging of 30 consecutive complexes for both the reference and estimated signal. This approach was inspired by the ST analyzers used in clinical practice.
    3. Determination of positions and amplitudes of R peak, S peak, and T wave in averaged complexes. These positions were also detected by CWT detector but with different settings.
    4. Determination of ST analysis for individual complexes by calculating the T/QRS ratio, i.e. the ratio of the amplitude of the T wave to the sum of the amplitude of the R and S waves.
    5. Plotting the determined values into the graph in the form of marks '*', as displayed by ST in the clinical practice.

4. Results

This section summarizes the results obtained when testing the hybrid method on real recordings. The statistical results obtained according to the ACC, SE, PPV and F1 indices are presented for the FECGDARHA database in Table 5. Indices values greater than 95% are highlighted in green (6 recordings evaluated according to ACC, 9 recordings evaluated according to SE, 11 recordings evaluated according to PPV, and 10 recordings evaluated according to F1). The values of all quality indices were higher than 80% with all recordings except r11 (indices values lower than 80% are highlighted in red). As for recordings r01, r05, r08 and r09, all fetal R-peaks were detected correctly; no FP or FN fetal R-peaks were detected, and all quality indices achieved a value of 100%. The table also shows the error mean values μ and values of $\pm 1.96\sigma$, reflecting the differences between the reference fHR and the fHR estimated by the hybrid method. The results can be interpreted as follows: the hybrid method was effective for all recordings (highlighted in green) except r11, since, in this case, high mean values μ and values of $\pm 1.96\sigma$ were obtained (highlighted in red).

The statistical evaluation for the Challenge database is summarized in Table 6. Indices values greater than 95% are highlighted in green (11 recordings evaluated according to ACC, 14 recordings evaluated according to SE and F1, and 15 recordings evaluated according to PPV). The ACC, SE and F1 parameters exceeded the value of 80% for 17 recordings, and PPV was higher than 80% for 20 recordings (indices values lower than 80% are highlighted in red). All fetal R-peaks were detected correctly in recordings a04, a05, a08, a15, a17, a22 and a25; in addition, no FP and FN values were detected, and values of 100% were achieved for all quality indices. When evaluating mean values μ and values of $\pm 1.96\sigma$, the method was effective for 15 and 13 recordings, respectively (highlighted in green). High mean values μ and values of $\pm 1.96\sigma$ were acquired for 10 and 12 recordings, respectively (highlighted in red).

The obtained results of parameters μ and $\pm 1.96\sigma$ can be visualized using Bland–Altman plots. These graphs carry the same information as mentioned in the previous paragraph, but in a graphical form. The example of Bland–Altman plots, (a) for recording r03 and (b) for recording r09 in Fig. 7, presents recordings for which highly accurate results were achieved in determining fHR. Fig. 8 shows (a) recording r04 and (b) recording r12, for which a slight deviation of fHR values from the reference values was achieved. Fig. 9 represents (a) recording a09 and (b) recording a16, for which the hybrid method was not effective because the estimated fHR values excessively deviated from the reference values.

A comparison of fHR traces of all recordings from the FECGDARHA database is shown in Fig. 10(a). All recordings except recording r11 copy the reference trend, and the method can, therefore, be considered effective for these recordings. As for the

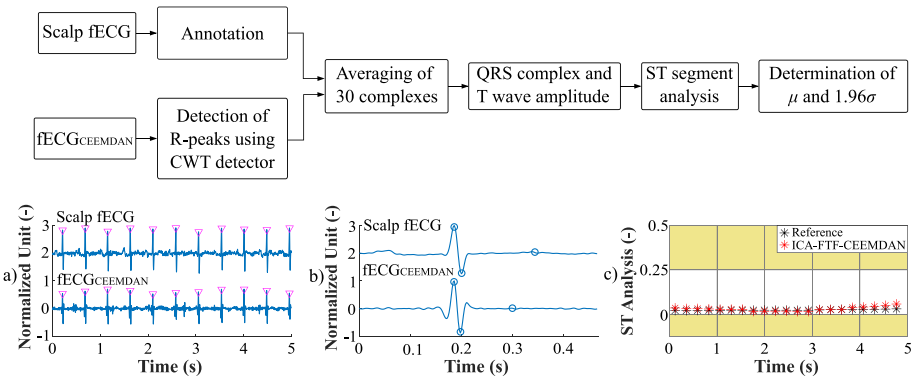

Fig. 6. Procedure of the ST segment analysis. Example (a) shows the extracted $fECG_{CEEMDAN}$ signal using a hybrid algorithm with detected R-peaks and reference signal. Example (b) shows averaged complex of extracted $fECG_{CEEMDAN}$ signal and reference recording with marked R peak, S peak and T wave locations. Example (c) represents graphical form of the ST segment analysis using the '*' marks.

Table 5
Statistical evaluation of the accuracy of fetal R-peaks detection and determination of fHR using the hybrid method when testing on the FECGDARHA database.

Recordings	Number of fetal R-peaks in annotations	TP	FP	FN	ACC (%)	SE (%)	PPV (%)	F1 (%)	μ (bpm)	$\pm 1.96\sigma$ (bpm)
r01	644	644	0	0	100.00	100.00	100.00	100.00	−0.18	5.32
r02	660	659	1	1	99.70	99.85	99.85	99.85	−0.01	7.64
r03	684	682	1	2	99.56	99.71	99.85	99.78	−0.02	2.58
r04	632	570	26	62	86.63	90.19	95.64	92.83	−1.90	7.50
r05	645	645	0	0	100.00	100.00	100.00	100.00	0.04	3.92
r06	674	643	20	31	92.65	95.40	96.98	96.19	−0.64	4.60
r07	627	595	18	32	92.25	94.90	97.06	95.67	−0.90	5.76
r08	651	651	0	0	100.00	100.00	100.00	100.00	−0.31	7.11
r09	657	657	0	0	100.00	100.00	100.00	100.00	0.03	2.52
r10	637	630	27	7	94.88	98.90	95.89	97.37	−0.12	7.10
r11	705	485	166	220	55.68	68.79	74.50	71.53	−7.14	21.67
r12	685	659	13	26	94.41	96.20	98.07	97.13	−1.11	8.50

Table 6
Statistical evaluation of the accuracy of fetal R-peaks detection and determination of fHR using the hybrid method when testing on the Challenge database.

Recordings	Number of fetal R-peaks in annotations	TP	FP	FN	ACC (%)	SE (%)	PPV (%)	F1 (%)	μ (bpm)	$\pm 1.96\sigma$ (bpm)
a01	145	139	4	6	93.30	95.86	97.20	96.53	0.01	10.82
a02	160	34	66	126	15.04	21.25	34.00	26.15	−36.64	22.95
a03	128	127	1	1	98.45	99.22	99.22	99.22	0.43	7.67
a04	129	129	0	0	100.00	100.00	100.00	100.00	−0.01	16.50
a05	129	129	0	0	100.00	100.00	100.00	100.00	0.01	1.63
a06	160	106	24	54	57.61	66.25	81.54	73.10	−16.35	18.89
a07	130	70	47	60	39.55	53.85	59.83	56.68	3.58	16.48
a08	128	128	0	0	100.00	100.00	100.00	100.00	0.04	1.83
a09	130	92	16	38	63.01	70.77	85.19	77.31	−8.44	15.07
a10	175	149	11	26	80.11	85.14	93.13	88.96	−9.09	13.05
a11	140	79	22	61	48.77	56.43	78.22	65.56	−19.47	19.28
a12	138	134	2	4	95.71	97.10	98.53	97.81	0.08	5.31
a13	126	121	2	5	94.53	96.03	98.38	97.19	−1.11	6.06
a14	123	121	1	2	97.58	98.37	99.18	98.78	−0.25	6.32
a15	134	134	0	0	100.00	100.00	100.00	100.00	0.07	12.24
a16	130	63	34	67	38.42	48.46	64.95	55.51	−13.14	18.49
a17	132	132	0	0	100.00	100.00	100.00	100.00	0.08	5.59
a18	150	31	66	119	14.35	20.67	31.96	25.10	−43.81	16.54
a19	127	122	4	5	93.13	96.06	96.83	96.44	−0.09	2.13
a20	131	121	4	10	89.63	92.37	96.80	94.53	−2.54	8.97
a21	145	102	11	43	65.39	70.35	90.27	79.07	−14.34	15.46
a22	126	126	0	0	100.00	100.00	100.00	100.00	0.05	2.03
a23	126	108	7	18	81.20	85.71	93.91	89.63	−4.39	7.70
a24	123	120	2	3	96.00	97.56	98.36	97.96	−0.17	3.98
a25	125	125	0	0	100.00	100.00	100.00	100.00	−0.01	3.19

recording r11, the method curve is deviated from the reference curve, and the determination of fHR using the hybrid method cannot be considered sufficiently accurate. A comparison of fHR traces of 12 selected recordings is shown in Fig. 10(b). In this case, the method was also effective for all displayed recordings, except for recording a23. Here, as in the previous case, this is a deviation of the method curve from the reference curve, which indicates an inaccurate estimate of fHR using the hybrid method. In both graphs, the names of the recordings are indicated at the top, and the sections related to the given recordings are marked with an arrow.

We also performed an ST analysis using the estimated data and evaluated its accuracy. The evaluation was based on a comparison of the T/QRS ratios estimated by the ICA-FTF-CEEMDAN method

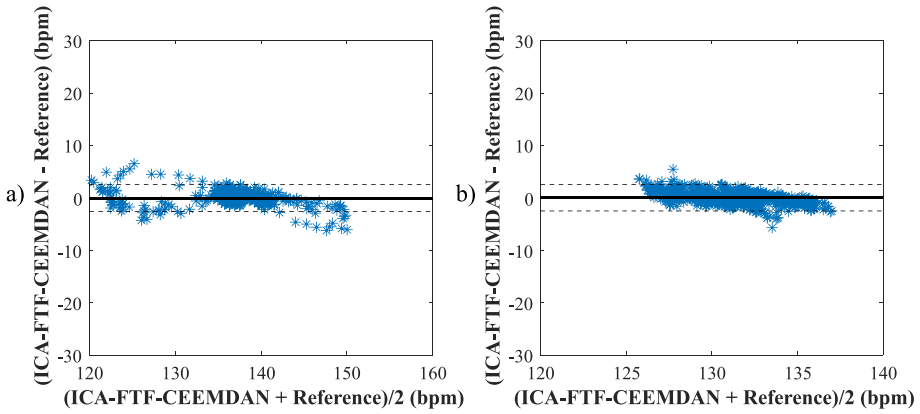

Fig. 7. Comparison of reference and estimated fHR values using the ICA-FTF-CEEMDAN method (a) for recording r03 and (b) for recording r09 using Bland–Altman plots.

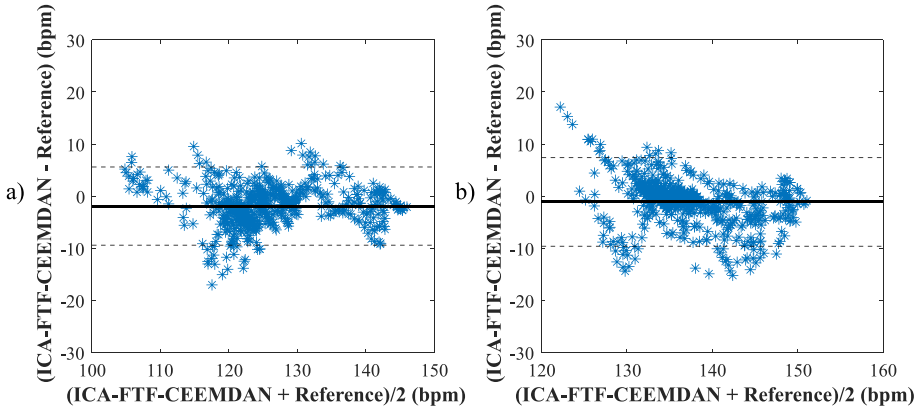

Fig. 8. Comparison of reference and estimated fHR values using the ICA-FTF-CEEMDAN method (a) for recording r04 and (b) for recording r12 using Bland–Altman plots.

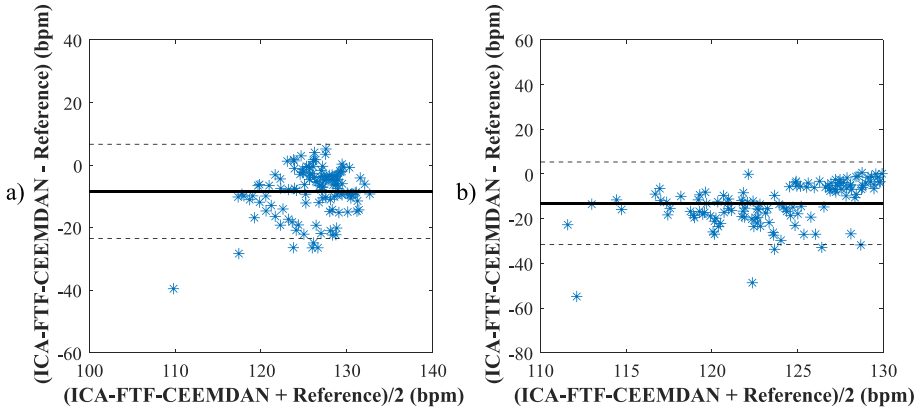

Fig. 9. Comparison of reference and estimated fHR values using the ICA-FTF-CEEMDAN method (a) for recording a09 and (b) for recording a16 using Bland–Altman plots.

compared to the ratios determined using the reference scalp fECG record. Since the reference record was only available in the FECGDARHA database, the ST analysis was performed on only 12 records from this database (the Challenge database contained only annotations with reference positions of fetal R-peaks). The values μ and $\pm 1.96\sigma$ were used for the comparison, see Table 7. According to the obtained results, ST analysis was performed with high accuracy (associated with low values of μ and $\pm 1.96\sigma$) for records r01, r02, r03, r05, r08, r09, and r10. High values of μ and $\pm 1.96\sigma$ were obtained for the remaining signals and therefore the ST analysis cannot be considered accurate.

The same conclusions can also be drawn when comparing the graphical outcomes of ST analysis on the estimated and reference fECG signals, see Fig. 11. For the records r01, r02, r03, r05, r08, r09, and r10, the values of the estimated T/QRS ratios are very close to the reference ones, while for the records r04, r06, r07, r11, and r12 it is the opposite case. For these records, the deviations are so significant that the red data points on the graph are not visible because they are outside the y-axis range. It can be concluded that ST segment analysis was highly effective in 7 of the 12 records tested. The inaccuracy of ST analysis for the

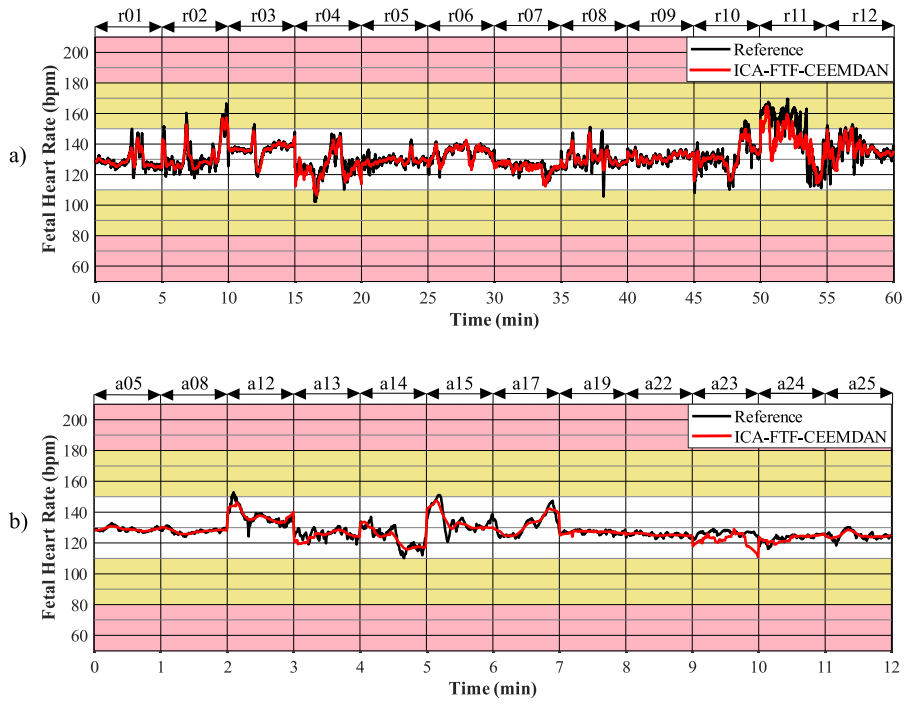

Fig. 10. Comparison of fHR traces extracted by ICA-FTF-CEEMDAN with references (a) for all recordings from the FECGDARHA database and (b) for 12 recordings from the Challenge database.

Table 7
Mean values μ and values of $\pm 1.96\sigma$ determined for ST analysis.

Recordings	μ (–)	$\pm 1.96\sigma$ (–)
r01	−0.0033	0.0043
r02	0.0285	0.0350
r03	0.0106	0.0146
r04	0.9227	1.6366
r05	0.0053	0.0195
r06	0.9568	1.7441
r07	4.1834	5.5388
r08	−0.0197	0.0046
r09	0.0252	0.0105
r10	0.0107	0.0064
r11	3.8900	4.6441
r12	12.7130	25.6508

remaining recordings could be due to poorer quality of the input aECG signals and less accurate detection of R oscillations.

In addition to evaluating filtering effectiveness, an evaluation of the algorithm was also performed in terms of the computational speed of the algorithm. A comparison of computational speed depending on filter order M using RLS and FTF algorithms is presented in Fig. 12(a), and a comparison of the computational speed as a function of the number of ensemble trials N of EEMD and CEEMDAN algorithms is shown in Fig. 12(b). An entire 5 min recording was used to evaluate the computational speed of the filter. The figure shows that the RLS and FTF filters worked at about the same speed up to the 20th filter order. At filter orders higher than this value, the RLS filter required approximately linearly more computation time, while the FTF filter was able to perform filtering quickly regardless of the filter order. As for the EEMD and CEEMDAN methods, there was a linear increase in computational time depending on the increasing number of ensemble trials N in both methods. However, the total computational time was approximately 40% lower for the CEEMDAN method.

5. Discussion

The results presented in this paper shows that the hybrid method was effective for most of the recordings tested. The method was not effective only for recordings that were not captured well. The influence of the quality of aECG signals on the resulting filtering is shown in Fig. 13. Example (a) presents recording r05, in which high accuracy was achieved in the detection of fQRS complexes (ACC = 100%). High-quality aECG signals were captured with this recording, without any significant interference and with sufficient fECG magnitude. While example (a) presents recording r11, in which low accuracy was achieved in the detection of fQRS complexes (ACC = 55.68%). The low effectiveness of this method was probably caused by the poor quality aECG signals, which contained interference and the fECG component acquired low magnitudes. Accurate extraction of fECG from such aECG signals is almost impossible.

In addition to the quality of aECG recordings, the resulting filter quality was also affected by the optimal setting of the parameters of the individual algorithms. As for the FTF algorithm, they are filtering order M and forgetting factor λ. The influence of setting these parameters for recording a24 is shown in Fig. 14. Example (a) shows the influence of setting these parameters on the resulting accuracy of fQRS complexes detection according to the ACC parameter in the form of a 3D graph. As for this recording, the filter was effective at the following setting: $\lambda > 0.9996$ and $46 < M < 54$. Example (b) shows the waveform of the signal where the setting was too low, $\lambda = 0.9995$ and $M = 44$, which led to a failure to suppress the mECG component, and, thus, to inaccurate detection of fQRS complexes (ACC = 65.52%). Example (c) shows the most effective signal extraction (ACC = 85.04%) where the optimal setting was achieved at $\lambda = 1$ and $M = 52$.

For the CEEMDAN method, the optimal setting of the number of ensemble trials N and the value of the standard deviation of the added noise series N_{std} affected the resulting filtration quality. The influence of setting these parameters also for recording a24 is shown in Fig. 15. Example (a) shows the influence of setting

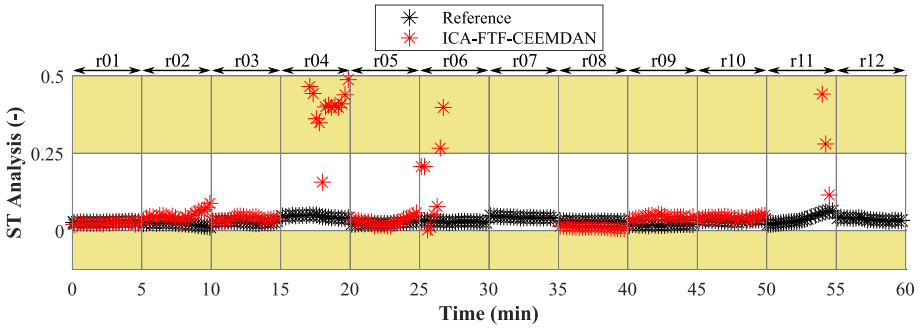

Fig. 11. Graphical illustration of the ST segment analysis based on the visualization used by the ST analyzers in the clinical practice.

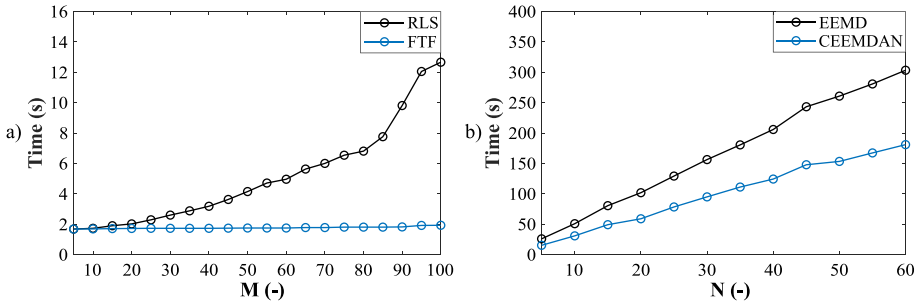

Fig. 12. A comparison of computational speed (a) depending on filter order M for RLS and FTF and (b) depending on the number of ensemble trials N for EEMD and CEEMDAN.

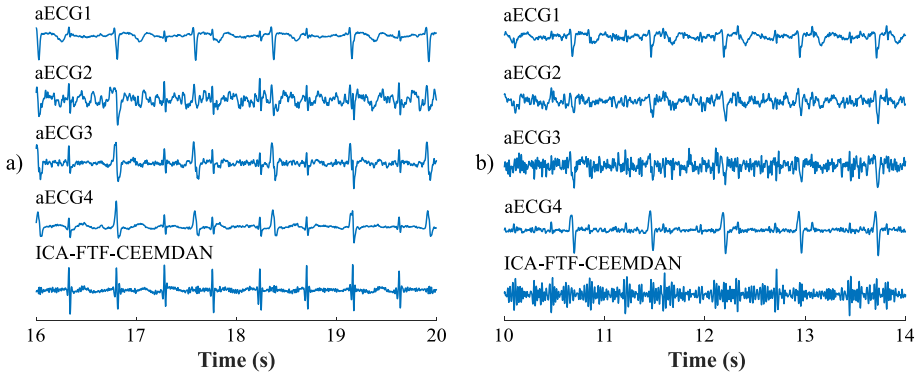

Fig. 13. Comparison of the influence of (a) good quality aECG signals on the resulting filtration quality (recording r05) (b) poor quality aECG signals containing noise and the fECG component having a low magnitude (recording r11).

these parameters on the resulting accuracy of fQRS complexes detection according to the ACC parameter in the form of a 3D graph. As for this recording, the filter was effective at the following setting: $N > 50$ and $N_{std} > 0.7$. Example (b) shows the waveform of the signal where the setting was too low, $N = 10$ and $N_{std} = 0.2$, which led to insufficient suppression of the mECG component, and, thus, to less accurate detection of fQRS complexes (ACC = 85.38%). Example (c) shows the most effective signal extraction (ACC = 96.00%) where the optimal setting was achieved at $N = 60$ and $N_{std} = 0.9$.

An example of a signal extracted using the ICA-FTF-CEEMDAN hybrid method in comparison with signals extracted using the other hybrid methods is shown in Fig. 16. It is visible that no significant differences in extraction quality are seen for the signals extracted using ICA-RLS and ICA-FTF. While using ICA-RLS-EEMD and ICA-FTF-CEEMDAN, the CEEMDAN method was able to suppress the maternal component slightly better. Moreover, the morphology of the fECG curve was not deformed as opposed to using the EEMD method.

Finally, we created both subjective and objective evaluation and summaries of other significant results in the field of fECG extraction. In this comparison, we tried to reflect key aspects, such as the algorithm used, the database on which the algorithm was tested, the accuracy of fetal R-peaks detection using ACC, SE, PPV, F1 statistical parameters (the average value for all recordings on which the method was tested) and the advantages and limitations of the methods, see Table 8.

- In a previous publication [95], a combination of sequential total variation denoising (STVD) and template subtraction using PCA (TSPCA) was tested on 8 recordings from the Fetal ECG Synthetic Database (FECGSYNDB) [96] and on 68 recordings from the Challenge 2013database. The evaluation of the accuracy of fetal R-peaks detection was assessed using the SE, PPV and F1 parameters, but only for recordings from the Challenge database. The authors achieved the following average values: SE = 90.50%, PPV = 89.40% and F1 = 89.90%, which are better results than those obtained in this study when testing on the Challenge database, but, on the

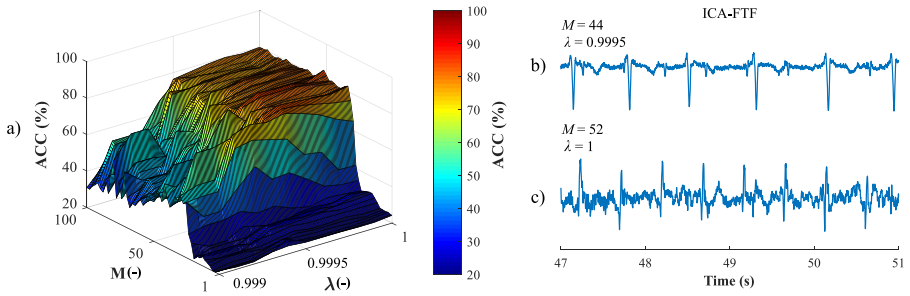

Fig. 14. Influence of parameter settings in the FTF method on the resulting quality of the extracted fECG signal. Illustration of the influence of filter order M and forgetting factor λ on the final extraction quality according to the ACC (a) by means of a 3D graph, (b) using the waveform of the extracted signal where the setting was too low, and (c) using the waveform of the extracted signal where the optimal setting was achieved.

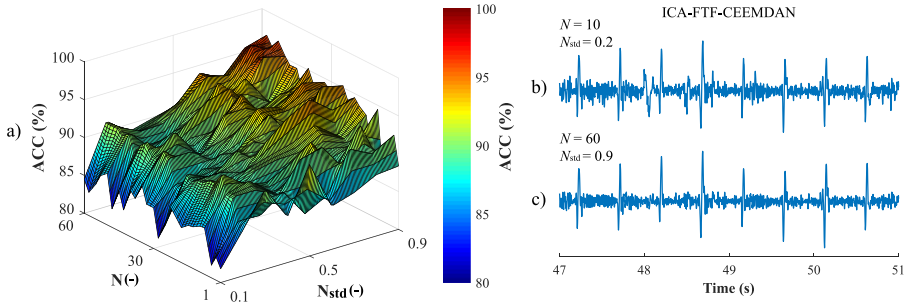

Fig. 15. Influence of parameter settings in the CEEMDAN method on the resulting quality of the extracted fECG signal. Illustration of the influence of number of ensemble trials N and the value of standard deviation of the added noise series N_{std} on the final extraction quality according to the ACC (a) by means of a 3D graph, (b) using the waveform of the extracted signal where the setting was too low, and (c) using the waveform of the extracted signal where the optimal setting was achieved.

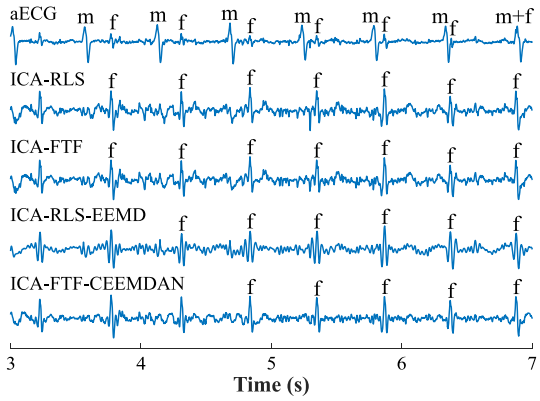

Fig. 16. An example of r10 signal extracted using the ICA-FTF-CEEMDAN hybrid method in comparison with signals extracted using the other hybrid methods, and an example of the input aECG signal.

other hand, worse than when testing on the FECGDARHA database. Its low computational burden enabling real-time monitoring was the advantage of the method. Its low performance in noisy signals and distortion of the morphology of the fECG signal were, however, the disadvantages of the method.

- The authors in [97] designed a combination of compressive sensing (CS) and non-negative matrix factorization (NMF), which they tested on 60 recordings from the Challenge 2013 database and 5 recordings from the Abdominal and Direct Fetal ECG Database (ADFECGDB), which is available at PhysioNet [91]. The ADFECGDB database contains 5 identical recordings (r01, r04, r07, r08 and r10) as well as the FECGDARHA database. In the ADFECGDB database, the average values of SE = 95.30%, PPV = 94.60% and F1 = 94.80% were achieved when evaluating the accuracy of fetal R-peaks detection, which are worse results than has been achieved in the current paper. For the Challenge database, only the average F1 was evaluated, which was also slightly lower (F1 = 84.00%) than the results reported here. In addition, the method did not work effectively with recordings with higher noise levels.
- A combination of periodic component analysis (πCA) and generalized eigenvalue decomposition (GEVD) was tested in [98] on recordings from the Database for the Identification of Systems (DaISy) [99]. The authors did not use any statistical parameters for the evaluation, but according to a visual comparison of the extracted signals, it can be argued that the method was able to extract fECG as effectively as the method proposed in the present paper.
- In [100], a combination of WT and a clustering-based technique (CT) was tested on 5 recordings from the ADFECGDB database and 26 recordings from the Challenge 2013 database. When testing on recordings from the ADFECGDB database, average values of ACC = 97.30%, SE = 98.40%, PPV = 98.40% and F1 = 98.63% were achieved when detecting fetal R-peaks. When testing on recordings from the Challenge database, the average values of ACC = 97.08%, SE = 97.93%, PPV = 99.11% and F1 = 98.52% were achieved, which, in both cases, are better results than we achieved. However, the authors excluded lower quality recordings.
- The authors in [101] combined the Savitzky–Golay smoothing filter (SGSF) and polynomial networks (PN). The method was tested on recordings from the Non-Invasive Fetal ECG Database (NIFECGDB) available on the PhysioNet [91]. The authors used a signal to noise ratio (SNR) – a different metric than what was used in the current study – to evaluate the extraction, but the residues of the mECG component were visible in the extracted signals, and it can therefore be argued that the method worked less effectively than the method we proposed.

- The combination of clustering and PCA was tested in [102] on 5 recordings from the ADFECGDB database, on 20 recordings from the Challenge 2013 database, and on recordings from the FECGSYNDB database containing abnormalities. When testing on recordings from the ADFECGDB database, average values of SE = 96.60%, PPV = 95.60% and F1 = 96.09% were achieved for detecting fetal R-peaks. When testing on recordings from the Challenge database, the average values of SE = 95.85%, PPV = 95.10% and F1 = 95.47% were achieved, which, in both cases, are better results than those obtained in the present study. The evaluation of the FECGSYNDB recordings was performed using the SNR parameter.
- In [103], a combination of CS and ICA was tested on 5 recordings from the ADFECGDB database and on recordings from the Challenge 2013 database. When testing on recordings from the ADFECGDB database, average values of SE = 92.50%, PPV = 92.00% and F1 = 92.20% were achieved for detecting fetal R-peaks. When testing on recordings from the Challenge database, average values of SE = 78.00%, PPV = 77.00% and F1 = 77.50% were achieved, which are worse results for both databases than those achieved using the algorithm proposed in the present paper.
- The authors in [104] tested a combination of extended Kalman smoother (EKS), ANFIS and differential evolution (DE) on 75 recordings from the Challenge 2013 database and 55 recordings from the NIFECGDB database. When testing on recordings from the Challenge database, average values of ACC = 84.89%, SE = 91.47%, PPV = 92.18% and F1 = 91.82% were achieved for detecting fetal R-peaks. When testing on recordings from the NIFECGDB database, the average values of ACC = 90.66%, SE = 94.21%, PPV = 96.05% and F1 = 95.12% were achieved. In both cases, these are better results than those obtained in the present study, but the authors state that worse fECG extraction could occur at a lower sampling frequency.
- The combination of RR time-series smoothing (RRTSS) and template-matching (TM) was tested in [34] on recordings from the Challenge 2013 database. When detecting fetal R-peaks, the average value of F1 = 95.00% was achieved. However, during the extraction, the fQRS complex was distorted, which would affect a deeper morphological analysis of the signal.
- Finally, we compared the achieved results with our previously presented algorithms. The algorithms were tested on the same databases (FECGDARHA database and Challenge 2013 database), and the results were evaluated using the same statistical parameters (ACC, SE, PPV, and F1). In [22], the ICA-RLS-WT algorithm was introduced. According to the statistical evaluation, worse results were achieved for recordings from both databases (FECGDARHA: ACC = 85.92%, SE = 89.70%, PPV = 92.41%, and F1 = 90.99%, Challenge 2013: ACC = 68.25%, SE = 72.60%, PPV = 81.31%, and F1 = 75.68%) than those achieved using the algorithm proposed in the present paper. Using the WT method, the algorithm was computationally less complex, but the morphology of the fQRS was distorted. In [46], the ICA-RLS-EMD algorithm was tested. According to the statistical evaluation, worse results were achieved for recordings from both databases (FECGDARHA: ACC = 84.73%, SE = 87.99%, PPV = 92.72%, and F1 = 90.10%, Challenge 2013: ACC = 64.95%, SE = 69.34%, PPV = 79.62%, and F1 = 72.74%) than those achieved using the new algorithm. Using the EMD method, the algorithm was computationally less complex (compared to the EEMD or CEEMDAN method), but it was less effective for recordings with low fECG magnitude.

6. Summary and future directions

Based on both objective and subjective evaluation, the proposed hybrid algorithm proved to be very efficient for signal extraction when tested on both publicly available databases. When testing on the FECGDARHA database, average values of ACC = 92.98%, SE = 95.33%, PPV = 96.49% and F1 = 95.86% for detection fQRS were achieved. The error in estimating the fHR was -1.02 ± 7.02 ($\mu\pm1.96\sigma$) bpm. When testing on the Challenge 2013 database, average values of ACC = 78.47%, SE = 82.06%, PPV = 87.90% and F1 = 84.62% for fQRS detection were achieved, and the error in estimating the fHR was -6.62 ± 10.33 ($\mu \pm 1.96\sigma$) bpm.

In addition, non-invasive ST analysis was performed on records from the FECGDARHA database, which was accurate in 7 of 12 records with values of $\mu < 0.03$ and values of $\pm1.96\sigma < 0.04$. A less accurate performance of ST analysis was for recordings whose aECG signals were not recorded in sufficient quality and for which the detection of R oscillations was less accurate. The dependence of the performance quality on the parameters setting can be considered as a limitation of the algorithm. The main benefits of the algorithm can be summarized as follows:

- Use of solely abdominal electrodes – it is thus not necessary to use a chest lead to obtain the reference mECG signal; this approach provides more comfort and mobility for the mother.
- High quality extraction of fECG thanks to the adaptive filter used.
- Accurate detection of fQRS complexes and determination of fHR.
- Preservation of signal morphology allowing accurate ST analysis.
- Time-efficient algorithm enabling implementation in real-time devices.

The proposed algorithm will be implemented within the prototype of a device for non-invasive fECG monitoring, on which our team is currently working. Using the device, it will be possible to record multichannel fECG signals and monitor fHR continuously. The device will be particularly suitable for remote home monitoring as a supplement to conventional CTG used in clinical practice.

If this device for non-invasive fECG monitoring and signal analysis based on ICA-FTF-CEEMDAN became a common part of clinical practice, or even replaced CTG, fetal hypoxia could be detected with greater accuracy compared to CTG due to accurate morphological signal analysis. This could lead to a significant reduction in the number of unnecessary caesarian sections. Reducing the number of these highly invasive procedures could lead to less mental and physical strain on the mother (for example, post-traumatic stress disorder, abnormal uterine bleeding or urinary incontinence have been reported in connection with cesarean section in the literature [105,106]). Another effect could be a reduction in the financial costs of health care providers (for example, due to longer postpartum care due to postpartum complications [107]). In addition, neither the mother nor the fetus would be exposed to emitted ultrasound energy, as is the case with CTG. Moreover, the measurements would not require highly skilled personnel thus it could be performed even in the comfort of home as part of remote monitoring. Compared to the invasive variant of fECG, the measurement would not only have to be performed during childbirth, but also during pregnancy, when heart disorders (for example, arrhythmias) could be detected well in advance. Furthermore, the fetus would not face the increased risk of injury to scalp by the scalp electrode associated with possibility of introducing an infection [108]. In addition to fECG

Table 8
Comparison of the results with other studies. ACC, SE, PPV, and F1 values shown are average values calculated for all recordings tested.

Author, source	Algorithm	Dataset	ACC (%)	SE (%)	PPV (%)	F1 (%)	Advantages and limitations
Lee et al. [95]	STVD-TSPCA	Challenge 2013 FECGSYNDB	– –	90.50 –	89.40 –	89.90 –	+ low computational load − distortion of fECG morphology − poor performance for low SNR levels
Gurve et al. [97]	CS-NMF	ADFECGDB Challenge 2013	95.30 –	94.60 –	94.80 –	84.00 –	+ single channel method − poor performance for high noise recordings
Sameni et al. [98]	πCA-GEVD	DaISy	–	–	–	–	+ time-efficient method − not tested on recordings with higher noise level
Castillo et al. [100]	WT-CT	ADFECGDB Challenge 2013	97.30 97.08	98.40 97.93	98.86 99.11	98.63 98.52	+ allows use in real time applications + single channel method − lower quality recordings were not used for testing
Ayat et al. [101]	SGSF-PN	NIFECGDB	–	–	–	–	+ single channel method − not tested on recordings with higher noise level
Zhang et al. [102]	Clustering-PCA	ADFECGDB Challenge 2013 FECGSYNDB	– – –	96.60 95.85 –	95.60 95.10 –	96.09 95.47 –	+ single channel method + tested on recordings with abnormalities − poor performance for high noise recordings
Da Poian et al. [103]	CS-ICA	ADFECGDB Challenge 2013	– –	92.50 78.00	92.00 77.00	92.20 77.50	+ allows use in real time applications + suitable for low-power monitoring devices − not effective for poor quality aECG signals
Panigrahy et al. [104]	EKS-DE-ANFIS	Challenge 2013 NIFECGDB	84.89 90.66	91.47 94.21	92.18 96.05	91.82 95.12	+ single channel method − low performance at lower sampling frequency
Liu et al. [34]	RRTSS-TM	Challenge 2013	–	–	–	95.00	+ single channel method − poor performance for high noise recordings − phase and amplitude of fQRS were distorted
Previously presented algorithm [22]	ICA-RLS-WT	FECGDARHA Challenge 2013	85.92 68.25	89.70 72.60	92.41 81.31	90.99 75.68	+ lower computational load due to the use of WT − distorts the morphology of fQRS
Previously presented algorithm [46]	ICA-RLS-EMD	FECGDARHA Challenge 2013	84.73 64.95	87.99 69.34	92.72 79.62	90.10 72.74	+ lower computational load due to the use of EMD − poor performance for recordings with low fECG magnitude
Proposed algorithm	ICA-FTF-CEEMDAN	FECGDARHA Challenge 2013	92.98 78.47	95.33 82.06	96.49 87.90	95.86 84.62	+ does not distort the morphology of fQRS − the need for optimal parameter settings

signals, electrical signals produced by uterus during contractions could be extracted and analyzed from the recordings.

The computational complexity of individual ICA and FTF methods was classified as low and the CEEMDAN method as a *medium* (see, Table 2), and thus the implementation within real-time devices appears to be very promising. However, the disadvantage of the algorithm was its dependence of high performance on optimal setting of parameters. Parameter optimization leads to an increase in the computational time of the algorithm. Therefore, if necessary to reduce the computational time, it is possible to reduce the time when optimizing the parameters as follows: (1) The algorithm setting could be optimized for a shorter signal section (such with 15, 30 or 60 s) and extraction would be performed with this setting for the rest of the signal; (2) The optimization could be also performed at shorter but more frequent intervals (for example, the first 10 s of the signal would be used for optimization, the next 60 s of the signal would be extracted with this setting followed by another 10 s for optimization, etc.).

The algorithm could also find application in other areas where it seems promising to use adaptive algorithms. These include the processing of other human biological signals, such as adult ECG [109,110], speech signals [111,112] or signals used in telecommunications [113].

Future research will focus on verifying the effectiveness of the method in the above-mentioned real prototype device and its effectiveness will be tested on a larger number of records, including pathological records. Using the prototype, a dataset will be created with real fECG records, both physiological and pathological, including different gestational gestation ages and fetal positions. In addition to non-invasive aECG recordings, a simultaneously recorded CTG reference or direct fECG signal using a scalp electrode so that we can create annotations. The dataset can then be used by researchers to evaluate the accuracy of filtration techniques. In the future, it is also possible to perform other types of morphological analyzes (such as QT interval analysis), which provide physicians with valuable information about the health of the fetus. Further research should also focus on the classification of fECG signals into categories, such as physiological and pathological, and on the detection of arrhythmias, as in the case of adult ECG [114,115]. Here, it would be appropriate to

test algorithms based on artificial intelligence and machine learning (e.g. ANNs, k-means, k-medoids, support vector machines or fuzzy logic) within the classification tasks.

7. Conclusion

The results of the study showed that the ICA-FTF-CEEMDAN hybrid method was able to efficiently extract fECG from abdominal recordings. Also, it achieved more accurate statistical results in the detection of fQRS complexes than the previously presented approaches. Compared to the RLS algorithm, the detection of fQRS complexes by FTF did not improve significantly. However, with increasing filter order, the RLS filter required linearly more computation time, while the FTF filter was able to perform filtering quickly regardless of the filter order (the computation time was approximately 2 s for filter order values ranging from 1 to 100). When comparing the EEMD and CEEMDAN methods, the CEEMDAN method achieved slightly better suppression of the maternal component. Further, the shape of the fECG waveform was not as deformed as when using EEMD. Preservation of the signal morphology has a fundamental influence on the subsequent morphological analysis of the fECG signal. As for both methods, there was a linear increase in computational time for both methods depending on the increasing number of ensemble trials in both methods, but the total computational time for the CEEMDAN method was approximately 40% lower. The proposed algorithm thus proved to be effective both in terms of accuracy of fHR determination and in terms of computational speed, i.e. enabling its implementation within real-time operating devices. Moreover, no additional lead is needed to record the reference mECG from the mother's chest, leading to greater maternal comfort and mobility. The main benefit of this approach is that it can obtain the signal of a sufficient quality to perform an accurate ST analysis. This confirms the assumption that non-invasive fECG monitoring can achieve as accurate results as when monitored invasively. Thus, non-invasive fECG appears to be a promising alternative to CTG and invasive fECG, which are used in the today's clinical practice. To verify the effectiveness of this combined algorithm, it would be necessary to have a database with a larger number of signals. Unfortunately, there are still relatively a few databases with real recordings and annotations. Therefore, future research will focus on the design of a monitoring device for fECG, where this algorithm will be tested on our own data. Furthermore, the algorithm will also be tested on pathological recordings, and the research will also focus on the classification of fECG signals into categories, such as physiological and pathological and other types of morphological analysis (such as QT interval analysis).

CRediT authorship contribution statement

Katerina Barnova: Methodology, Investigation, Validation, Writing – original draft. **Radek Martinek:** Conceptualization, Supervision, Funding acquisition. **Rene Jaros:** Software, Visualization, Data curation. **Radana Kahankova:** Investigation, Validation, Formal analysis, Editing. **Khosrow Behbehani:** Writing – review & editing. **Vaclav Snasel:** Project administration, Supervision, Validation.

Declaration of competing interest

The authors declare that they have no known competing financial interests or personal relationships that could have appeared to influence the work reported in this paper.

Acknowledgment

This article was supported by the Ministry of Education of the Czech Republic (Projects No. SP2021/32, SP2021/24). This article was also supported by the European Regional Development Fund in the Research Centre of Advanced Mechatronic Systems project, project number CZ.02.1.01/0.0/0.0/16_019/0000867 within the Operational Programme Research, Development and Education.

References

[1] D. Hutter, J. Kingdom, E. Jaeggi, Causes and mechanisms of intrauterine hypoxia and its impact on the fetal cardiovascular system: a review, Int. J. Pediatrics 2010 (2010) 1–9, http://dx.doi.org/10.1155/2010/401323.

[2] L.J. Millar, L. Shi, A. Hoerder-Suabedissen, Z. Molnár, Neonatal hypoxia ischaemia: mechanisms, models, and therapeutic challenges, Front. Cell. Neurosci. 11 (2017) 78, http://dx.doi.org/10.3389/fncel.2017.00078.

[3] J. Samuel, C. Franklin, Hypoxemia and hypoxia, in: J.A. Myers, K.W. Millikan, T.J. Saclarides (Eds.), Common Surgical Diseases, Springer New York, New York, NY, 2008, pp. 391–394, http://dx.doi.org/10.1007/978-0-387-75246-4_97.

[4] S. Vannuccini, C. Bocchi, F.M. Severi, F. Petraglia, Diagnosis of fetal distress, in: G. Buonocore, R. Bracci, M. Weindling (Eds.), Neonatology, Springer International Publishing, Cham, 2016, pp. 1–23, http://dx.doi.org/10.1007/978-3-319-18159-2_156-1.

[5] M. Herrera-Marschitz, T. Neira-Pena, E. Rojas-Mancilla, P. Espina-Marchant, D. Esmar, R. Perez, V. Muãoz, M. Gutierrez-Hernandez, B. Rivera, N. Simola, D. Bustamante, P. Morales, P.J. Gebicke-Haerter, Perinatal asphyxia: CNS development and deficits with delayed onset, Front. Neurosci. 8 (2014) http://dx.doi.org/10.3389/fnins.2014.00047.

[6] W. Künzel (Ed.), Fetal Heart Rate Monitoring: Clinical Practice and Pathophysiology, Springer Berlin Heidelberg, Berlin, Heidelberg, 1985, http://dx.doi.org/10.1007/978-3-642-70358-4.

[7] C. Smyth, J. Farrow, Present place in obstetrics for foetal phonocardiography and electrocardiography, BMJ (Clin. Res. Ed.) 2 (5103) (1958) 1005–1009, http://dx.doi.org/10.1136/bmj.2.5103.1005.

[8] C.B. Martin, Electronic fetal monitoring: A brief summary of its development, problems and prospects, Eur. J. Obstet. Gynecol. Reprod. Biol. 78 (2) (1998) 133–140, http://dx.doi.org/10.1016/S0301-2115(98)00059-1.

[9] R. Kahankova, R. Martinek, R. Jaros, K. Behbehani, A. Matonia, M. Jezewski, J.A. Behar, A review of signal processing techniques for non-invasive fetal electrocardiography, IEEE Rev. Biomed. Eng. 13 (2020) 51–73, http://dx.doi.org/10.1109/RBME.2019.2938061.

[10] A. Pinas, E. Chandraharan, Continuous cardiotocography during labour: analysis, classification and management, Best Pract. Res. Clin. Obstet. Gynaecol. 30 (2016) 33–47, http://dx.doi.org/10.1016/j.bpobgyn.2015.03.022.

[11] T. Khangura, E. Chandraharan, Electronic fetal heart rate monitoring: the future, Curr. Women's Health Rev. 9 (3) (2014) 169–174, http://dx.doi.org/10.2174/1573404809031401311111807.

[12] S. Vannuccini, C. Bocchi, F.M. Severi, F. Petraglia, Diagnosis of fetal distress, in: G. Buonocore, R. Bracci, M. Weindling (Eds.), Neonatology, Springer International Publishing, Cham, 2018, pp. 105–127, http://dx.doi.org/10.1007/978-3-319-29489-6_156.

[13] R.L. Williams, W.E. Hawes, Cesarean section, fetal monitoring, and perinatal mortality in california., Am J Public Health 69 (9) (1979) 864–870, http://dx.doi.org/10.2105/AJPH.69.9.864.

[14] H.-Y. Chen, S.P. Chauhan, C.V. Ananth, A.M. Vintzileos, A.Z. Abuhamad, Electronic fetal heart rate monitoring and its relationship to neonatal and infant mortality in the United States, Am. J. Obstet. Gynecol. 204 (6) (2011) 491.e1–491.e10, http://dx.doi.org/10.1016/j.ajog.2011.04.024.

[15] A.P. Betrán, J. Ye, A.-B. Moller, J. Zhang, A.M. Gülmezoglu, M.R. Torloni, The increasing trend in caesarean section rates: global, regional and national estimates: 1990–2014, PLoS One 11 (2) (2016) e0148343, http://dx.doi.org/10.1371/journal.pone.0148343.

[16] E. Blix, K.G. Brurberg, E. Reierth, L.M. Reinar, P. Øian, ST waveform analysis versus cardiotocography alone for intrapartum fetal monitoring: A systematic review and meta-analysis of randomized trials, Acta Obstet. Gynecol. Scand. 95 (1) (2016) 16–27, http://dx.doi.org/10.1111/aogs.12828.

[17] T. Kazmi, F. Radfer, S. Khan, ST Analysis of the fetal ECG, as an adjunct to fetal heart rate monitoring in labour: a review, Oman Med. J. 26 (6) (2011) 459–460, http://dx.doi.org/10.5001/omj.2011.118.

[18] E. Karvounis, M. Tsipouras, C. Papaloukas, D. Tsalikakis, K. Naka, D. Fotiadis, A non-invasive methodology for fetal monitoring during pregnancy, Methods Inf. Med. 49 (03) (2010) 238–253, http://dx.doi.org/10.3414/ME09-01-0041.

[19] D. Jagannath, A.I. Selvakumar, Issues and research on foetal electrocardiogram signal elicitation, Biomed. Signal Process. Control 10 (2014) 224–244, http://dx.doi.org/10.1016/j.bspc.2013.11.001.
[20] Sameni, A review of fetal ECG signal processing issues and promising directions, the open pacing, Electrophysiol. Ther. J. (2010) http://dx.doi.org/10.2174/1876536X01003010004.
[21] G.D. Clifford, I. Silva, J. Behar, G.B. Moody, Non-invasive fetal ECG analysis, Physiol. Meas. 35 (8) (2014) 1521–1536, http://dx.doi.org/10.1088/0967-3334/35/8/1521.
[22] R. Jaros, R. Martinek, R. Kahankova, J. Koziorek, Novel hybrid extraction systems for fetal heart rate variability monitoring based on non-invasive fetal electrocardiogram, IEEE Access 7 (2019) 131758–131784, http://dx.doi.org/10.1109/ACCESS.2019.2933717.
[23] D.A. Ramli, Y.H. Shiong, N. Hassan, Blind source separation (BSS) of mixed maternal and fetal electrocardiogram (ECG) signal: A comparative study, Procedia Comput. Sci. 176 (2020) 582–591, http://dx.doi.org/10.1016/j.procs.2020.08.060.
[24] A. Ghazdali, A. Hakim, A. Laghrib, N. Mamouni, S. Raghay, A new method for the extraction of fetal ECG from the dependent abdominal signals using blind source separation and adaptive noise cancellation techniques, Theor. Biol. Med. Model. 12 (1) (2015) 25, http://dx.doi.org/10.1186/s12976-015-0021-2.
[25] P.J. He, X.M. Chen, Y. Liang, H.Z. Zeng, Extraction for fetal ECG using single channel blind source separation algorithm based on multi-algorithm fusion, in: W.-P. Sung, J. Kao (Eds.), MATEC Web Conf. 44 (2016) 01026, http://dx.doi.org/10.1051/matecconf/20164401026.
[26] R. Martinek, R. Kahankova, J. Jezewski, R. Jaros, J. Mohylova, M. Fajkus, J. Nedoma, P. Janku, H. Nazeran, Comparative effectiveness of ICA and PCA in extraction of fetal ECG from abdominal signals: toward non-invasive fetal monitoring, Front. Physiol. 9 (2018) 648, http://dx.doi.org/10.3389/fphys.2018.00648.
[27] P. Manorost, N. Theera-Umpon, S. Auephanwiriyakul, Fetal electrocardiogram extraction by independent component analysis, in: 2017 7th IEEE International Conference on Control System, Computing and Engineering (ICCSCE), IEEE, Penang, 2017, pp. 220–225, http://dx.doi.org/10.1109/ICCSCE.2017.8284408.
[28] M. Kotas, J. Giraldo, S.H. Contreras-Ortiz, G.I.B. Lasprilla, Fetal ECG extraction using independent component analysis by jade approach, in: J. Brieva, J.D. García, N. Lepore, E. Romero (Eds.), 13th International Conference on Medical Information Processing and Analysis, SPIE, San Andres Island, Colombia, 2017, p. 55, http://dx.doi.org/10.1117/12.2285962.
[29] R. Petrolis, V. Gintautas, A. Krisciukaitis, Multistage principal component analysis based method for abdominal ECG decomposition, Physiol. Meas. 36 (2) (2015) 329–340, http://dx.doi.org/10.1088/0967-3334/36/2/329.
[30] H. Hassanpour, A. Parsaei, Fetal ECG extraction using wavelet transform, in: 2006 International Conference on Computational Inteligence for Modelling Control and Automation and International Conference on Intelligent Agents Web Technologies and International Commerce (CIMCA'06), IEEE, Sydney, NSW, 2006, p. 179, http://dx.doi.org/10.1109/CIMCA.2006.98.
[31] Y. Alshebly, M. Nafea, Isolation of fetal ECG signals from abdominal ECG using wavelet analysis, IRBM 41 (5) (2020) 252–260, http://dx.doi.org/10.1016/j.irbm.2019.12.002.
[32] S. Wu, Y. Shen, Z. Zhou, L. Lin, Y. Zeng, X. Gao, Research of fetal ECG extraction using wavelet analysis and adaptive filtering, Comput. Biol. Med. 43 (10) (2013) 1622–1627, http://dx.doi.org/10.1016/j.compbiomed.2013.07.028.
[33] A. Matonia, J. Jezewski, K. Horoba, A. Gacek, P. Labaj, The maternal ECG suppression algorithm for efficient extraction of the fetal ECG from abdominal signal, in: 2006 International Conference of the IEEE Engineering in Medicine and Biology Society, IEEE, New York, NY, 2006, pp. 3106–3109, http://dx.doi.org/10.1109/IEMBS.2006.260221.
[34] H. Liu, D. Chen, G. Sun, Detection of fetal ECG r wave from single-lead abdominal ecg using a combination of RR time-series smoothing and template-matching approach, IEEE Access 7 (2019) 66633–66643, http://dx.doi.org/10.1109/ACCESS.2019.2917826.
[35] G. Camps, M. Martinez, E. Soria, Fetal ECG extraction using an FIR neural network, in: Computers in Cardiology 2001. Vol.28 (Cat. No.01CH37287), IEEE, Rotterdam, Netherlands, 2001, pp. 249–252, http://dx.doi.org/10.1109/CIC.2001.977639.
[36] G. Camps-Valls, M. Martínez-Sober, E. Soria-Olivas, R. Magdalena-Benedito, J. Calpe-Maravilla, J. Guerrero-Martínez, Foetal ECG recovery using dynamic neural networks, Artif. Intell. Med. 31 (3) (2004) 197–209, http://dx.doi.org/10.1016/j.artmed.2004.03.005.
[37] M. Bin Ibne Reaz, L.S. Wei, Adaptive linear neural network filter for fetal ECG extraction, in: International Conference on Intelligent Sensing and Information Processing, 2004. Proceedings of, IEEE, Chennai, India, 2004, pp. 321–324, http://dx.doi.org/10.1109/ICISIP.2004.1287675.
[38] R. Kahankova, R. Martinek, M. Mikolasova, R. Jaros, Adaptive linear neuron for fetal electrocardiogram extraction, in: 2018 IEEE 20th International Conference on E-Health Networking, Applications and Services (Healthcom), IEEE, Ostrava, 2018, pp. 1–5, http://dx.doi.org/10.1109/HealthCom.2018.8531135.
[39] L. Billeci, M. Varanini, A combined independent source separation and quality index optimization method for fetal ECG extraction from abdominal maternal leads, Sensors 17 (5) (2017) 1135, http://dx.doi.org/10.3390/s17051135.
[40] G. Liu, Y. Luan, An adaptive integrated algorithm for noninvasive fetal ECG separation and noise reduction based on ICA-EEMD-WS, Med. Biol. Eng. Comput. 53 (11) (2015) 1113–1127, http://dx.doi.org/10.1007/s11517-015-1389-1.
[41] A. Gupta, M. Srivastava, V. Khandelwal, A. Gupta, A novel approach to fetal ECG extraction and enhancement using blind source separation (BSS-ICA) and adaptive fetal ECG enhancer (AFE), in: 2007 6th International Conference on Information, Communications & Signal Processing, IEEE, Singapore, 2007, pp. 1–4, http://dx.doi.org/10.1109/ICICS.2007.4449716.
[42] R. Jaros, R. Martinek, K. Barnova, M. Ladrova, Use of a hybrid method ICA-PCA-ICA for fetal electrocardiography extraction, in: 2019 International Symposium on Advanced Electrical and Communication Technologies (ISAECT), IEEE, Rome, Italy, 2019, pp. 1–6, http://dx.doi.org/10.1109/ISAECT47714.2019.9069682.
[43] C. Li, B. Fang, H. Li, P. Wang, A novel method of FECG extraction combined self-correlation analysis with ICA, in: 2016 8th IEEE International Conference on Communication Software and Networks (ICCSN), IEEE, Beijing, China, 2016, pp. 107–111, http://dx.doi.org/10.1109/ICCSN.2016.7586629.
[44] V. Ionescu, Fetal ECG extraction from multichannel abdominal ECG recordings for health monitoring during labor, Proc. Technol. 22 (2016) 682–689, http://dx.doi.org/10.1016/j.protcy.2016.01.143.
[45] M. Hasan, M. Reaz, M. Ibrahimy, Fetal electrocardiogram extraction and r-peak detection for fetal heart rate monitoring using artificial neural network and correlation, in: The 2011 International Joint Conference on Neural Networks, IEEE, San Jose, CA, USA, 2011, pp. 15–20, http://dx.doi.org/10.1109/IJCNN.2011.6033193.
[46] K. Barnova, R. Martinek, R. Jaros, R. Kahankova, Hybrid methods based on empirical mode decomposition for non-invasive fetal heart rate monitoring, IEEE Access 8 (2020) 51200–51218, http://dx.doi.org/10.1109/ACCESS.2020.2980254.
[47] R. Martinek, R. Kahankova, H. Nazeran, J. Konecny, J. Jezewski, P. Janku, P. Bilik, J. Zidek, J. Nedoma, M. Fajkus, Non-invasive fetal monitoring: a maternal surface ECG electrode placement-based novel approach for optimization of adaptive filter control parameters using the LMS and RLS algorithms, Sensors 17 (5) (2017) 1154, http://dx.doi.org/10.3390/s17051154.
[48] R. Martinek, R. Kahankova, H. Skutova, P. Koudelka, J. Zidek, J. Koziorek, Adaptive signal processing techniques for extracting abdominal fetal electrocardiogram, in: 2016 10th International Symposium on Communication Systems, Networks and Digital Signal Processing (CSNDSP), IEEE, Prague, Czech Republic, 2016, pp. 1–6, http://dx.doi.org/10.1109/CSNDSP.2016.7573974.
[49] K.-A. Lee, W.-S. Gan, S.M. Kuo, Subband Adaptive Filtering: Theory and Implementation, J. Wiley, Chichester, U.K, 2009.
[50] S. Douglas, R. Losada, Adaptive filters in matlab: from novice to expert, in: Proceedings of 2002 IEEE 10th Digital Signal Processing Workshop, 2002 and the 2nd Signal Processing Education Workshop., IEEE, Pine Mountain, GA, USA, 2002, pp. 168–173, http://dx.doi.org/10.1109/DSPWS.2002.1231097.
[51] H. Kaur, R. Talwar, Performance comparison of adaptive filter algorithms for noise cancellation, in: 2013 International Conference on Emerging Trends in Communication, Control, Signal Processing and Computing Applications (C2SPCA), IEEE, Bangalore, India, 2013, pp. 1–5, http://dx.doi.org/10.1109/C2SPCA.2013.6749421.
[52] Z. Shengkui, M. Zhihong, K. Suiyang, A fast variable step-size LMS algorithm with system identification, in: 2007 2nd IEEE Conference on Industrial Electronics and Applications, IEEE, Harbin, China, 2007, pp. 2340–2345, http://dx.doi.org/10.1109/ICIEA.2007.4318828.
[53] P.S. Diniz, Conventional rls adaptive filter, in: Adaptive Filtering, Springer US, Boston, MA, 2008, pp. 1–36, http://dx.doi.org/10.1007/978-0-387-68606-6_5.
[54] J. Cioffi, T. Kailath, Fast, recursive-least-squares transversal filters for adaptive filtering, IEEE Trans. Acoust. Speech Signal Process. 32 (2) (1984) 304–337, http://dx.doi.org/10.1109/TASSP.1984.1164334.
[55] M. Setareh, M. Parniani, F. Aminifar, Non-stationary stabilized fast transversal RLS filter for online power system modal estimation, IEEE Trans. Power Syst. 34 (4) (2019) 2744–2754, http://dx.doi.org/10.1109/TPWRS.2019.2898168.
[56] A. Bessekri, M. Djendi, A. Guessoum, A new simplified fast transversal filter algorithm based on subband approach (SSFTF) for acoustic echo cancellation, Appl. Acoust. 161 (2020) 107178, http://dx.doi.org/10.1016/j.apacoust.2019.107178.
[57] S.-j. Liu, D.-l. Liu, J.-q. Zhang, Y.-j. Zeng, Extraction of fetal electrocardiogram using recursive least squares and normalized least mean squares algorithms, in: 2011 3rd International Conference on Advanced Computer Control, IEEE, Harbin, China, 2011, pp. 333–336, http://dx.doi.org/10.1109/ICACC.2011.6016426.

[58] J. Behar, A. Johnson, G.D. Clifford, J. Oster, A comparison of single channel fetal ECG extraction methods, Ann. Biomed. Eng. 42 (6) (2014) 1340–1353, http://dx.doi.org/10.1007/s10439-014-0993-9.

[59] S.L. Lima-Herrera, C. Alvarado-Serrano, P.R. Hernandez-Rodriguez, Fetal ECG extraction based on adaptive filters and wavelet transform: validation and application in fetal heart rate variability analysis, in: 2016 13th International Conference on Electrical Engineering, Computing Science and Automatic Control (CCE), IEEE, Mexico City, Mexico, 2016, pp. 1–6, http://dx.doi.org/10.1109/ICEEE.2016.7751243.

[60] S. Ziani, Y. El Hassouani, Fetal electrocardiogram analysis based on LMS adaptive filtering and complex continuous wavelet 1-d, in: Y. Farhaoui (Ed.), Big Data and Networks Technologies, Vol. 81, Springer International Publishing, Cham, 2020, pp. 360–366, http://dx.doi.org/10.1007/978-3-030-23672-4_26.

[61] A.M. Kaleem, R.D. Kokate, An efficient adaptive filter for fetal ECG extraction using neural network, J. Intell. Syst. 28 (4) (2019) 589–600, http://dx.doi.org/10.1515/jisys-2017-0031.

[62] R. Swarnalatha, D. Prasad, A novel technique for extraction of FECG using multi stage adaptive filtering, J. Appl. Sci. 10 (4) (2010) 319–324, http://dx.doi.org/10.3923/jas.2010.319.324.

[63] N.E. Huang, Z. Shen, S.R. Long, M.C. Wu, H.H. Shih, Q. Zheng, N.-C. Yen, C.C. Tung, H.H. Liu, The empirical mode decomposition and the Hilbert spectrum for nonlinear and non-stationary time series analysis, Proc. R. Soc. Lond. Ser. A Math. Phys. Eng. Sci. 454 (1971) (1998) 903–995, http://dx.doi.org/10.1098/rspa.1998.0193.

[64] Y. Ren, P. Suganthan, N. Srikanth, A comparative study of empirical mode decomposition-based short-term wind speed forecasting methods, IEEE Trans. Sustain. Energy 6 (1) (2015) 236–244, http://dx.doi.org/10.1109/TSTE.2014.2365580.

[65] S. Jha, O. Singh, R.K. Sunkaria, Modified approach for ECG signal denoising based on empirical mode decomposition and moving average filter, Int. J. Med. Eng. Inform. 6 (2) (2014) 165, http://dx.doi.org/10.1504/IJMEI.2014.060250.

[66] Y. Gao, G. Ge, Z. Sheng, E. Sang, Analysis and solution to the mode mixing phenomenon in EMD, in: 2008 Congress on Image and Signal Processing, IEEE, Sanya, China, 2008, pp. 223–227, http://dx.doi.org/10.1109/CISP.2008.193.

[67] Z. Wu, N.E. Huang, Ensemble empirical mode decomposition: a noise-assisted data analysis method, Adv. Adapt. Data Anal. 01 (01) (2009) 1–41, http://dx.doi.org/10.1142/S1793536909000047.

[68] K.-M. Chang, Ensemble empirical mode decomposition based ECG noise filtering method, in: 2010 International Conference on Machine Learning and Cybernetics, IEEE, Qingdao, China, 2010, pp. 210–213, http://dx.doi.org/10.1109/ICMLC.2010.5581064.

[69] J.-R. Yeh, J.-S. Shieh, N.E. Huang, Complementary ensemble empirical mode decomposition: a novel noise enhanced data analysis method, Adv. Adapt. Data Anal. 02 (02) (2010) 135–156, http://dx.doi.org/10.1142/S1793536910000422.

[70] M.E. Torres, M.A. Colominas, G. Schlotthauer, P. Flandrin, A complete ensemble empirical mode decomposition with adaptive noise, in: 2011 IEEE International Conference on Acoustics, Speech and Signal Processing (ICASSP), IEEE, Prague, Czech Republic, 2011, pp. 4144–4147, http://dx.doi.org/10.1109/ICASSP.2011.5947265.

[71] D.D. Taralunga, I. Gussi, R. Strungaru, A new method for fetal electrocardiogram denoising using blind source separation and empirical mode decomposition, Rev. Roum. Sci. Tech. Ser. Électrotech. Énerg. 61 (1) (2016) 94–98.

[72] X. Wei, W. Zheng, An integrated approach for fetal heart rate estimation from abdominal electrocardiogram signal, Chin. J. Electron. 28 (6) (2019) 1198–1203, http://dx.doi.org/10.1049/cje.2019.08.002.

[73] P. Ghobadi Azbari, M. Abdolghaffar, S. Mohaqeqi, M. Pooyan, A. Ahmadian, N. Ghanbarzadeh Gashti, A novel approach to the extraction of fetal electrocardiogram based on empirical mode decomposition and correlation analysis, Australas. Phys. Eng. Sci. Med. 40 (3) (2017) 565–574, http://dx.doi.org/10.1007/s13246-017-0560-4.

[74] P.R. Muduli, A. Mukherjee, Noise-assisted trend-filtering of fetal-electrocardiogram signals, in: 2016 IEEE EMBS Conference on Biomedical Engineering and Sciences (IECBES), IEEE, Malaysia, 2016, pp. 465–469, http://dx.doi.org/10.1109/IECBES.2016.7843494.

[75] A. Bin Queyam, S. Kumar Pahuja, D. Singh, Quantification of feto-maternal heart rate from abdominal ecg signal using empirical mode decomposition for heart rate variability analysis, Technologies 5 (4) (2017) 68, http://dx.doi.org/10.3390/technologies5040068.

[76] T. Liu, Z. Luo, J. Huang, S. Yan, A comparative study of four kinds of adaptive decomposition algorithms and their applications, Sensors 18 (7) (2018) 2120, http://dx.doi.org/10.3390/s18072120.

[77] M.A. Colominas, G. Schlotthauer, M.E. Torres, Improved complete ensemble EMD: A suitable tool for biomedical signal processing, Biomed. Signal Process. Control 14 (2014) 19–29, http://dx.doi.org/10.1016/j.bspc.2014.06.009.

[78] Y.-x. Li, L. Wang, A novel noise reduction technique for underwater acoustic signals based on complete ensemble empirical mode decomposition with adaptive noise, minimum mean square variance criterion and least mean square adaptive filter, Def. Technol. 16 (3) (2020) 543–554, http://dx.doi.org/10.1016/j.dt.2019.07.020.

[79] C.J. James, C.W. Hesse, Independent component analysis for biomedical signals, Physiol. Meas. 26 (1) (2005) R15–R39, http://dx.doi.org/10.1088/0967-3334/26/1/R02.

[80] V. Gupta, M. Mittal, V. Mittal, R-peak detection based chaos analysis of ECG signal, Analog Integr. Circuits Signal Process. 102 (3) (2020) 479–490, http://dx.doi.org/10.1007/s10470-019-01556-1.

[81] V. Gupta, M. Mittal, A comparison of ECG signal pre-processing using frft, frwt and IPCA for improved analysis, IRBM 40 (3) (2019) 145–156, http://dx.doi.org/10.1016/j.irbm.2019.04.003.

[82] G.R. Naik, D.K. Kumar, An overview of independent component analysis and its applications, Informatica 35 (1) (2011).

[83] J.J.R. Immanuel, V. Prabhu, V.J. Christopheraj, D. Sugumar, P. Vanathi, Separation of maternal and fetal ECG signals from the mixed source signal using FASTICA, Procedia Eng. 30 (2012) 356–363, http://dx.doi.org/10.1016/j.proeng.2012.01.872.

[84] D. Taralunga, M. Ungureanu, R. Strungaru, W. Wolf, Performance comparison of four ICA algorithms applied for fECG extraction from transabdominal recordings, in: ISSCS 2011 - International Symposium on Signals, Circuits and Systems, IEEE, Iasi, Romania, 2011, pp. 1–4, http://dx.doi.org/10.1109/ISSCS.2011.5978768.

[85] D. Slock, T. Kailath, Numerically stable fast transversal filters for recursive least squares adaptive filtering, IEEE Trans. Signal Process. 39 (1) (Jan./1991) 92–114, http://dx.doi.org/10.1109/78.80769.

[86] D.J. Dechene, Fast transversal recursive least-squares (FT-RLS) algorithm, in: IEEE Trans Signal Proc, Citeseer, 2007.

[87] Z. Ren, H. Schütze, A stabilized fast transversal filters algorithm for recursive least squares adaptive filtering, Signal Process. 39 (3) (1994) 235–246, http://dx.doi.org/10.1016/0165-1684(94)90087-6.

[88] K. Bensafia, A. Mansour, A.-O. Boudraa, S. Haddab, P. Ariès, B. Clement, Blind separation of ECG signals from noisy signals affected by electro-surgical artifacts, Analog Integr. Circuits Signal Process. 104 (2) (2020) 191–204, http://dx.doi.org/10.1007/s10470-020-01674-1.

[89] A. Hyvärinen, E. Oja, Independent component analysis: Algorithms and applications, Neural Netw. 13 (4–5) (2000) 411–430, http://dx.doi.org/10.1016/S0893-6080(00)00026-5.

[90] A. Matonia, J. Jezewski, T. Kupka, M. Jezewski, K. Horoba, J. Wrobel, R. Czabanski, R. Kahankova, Fetal electrocardiograms, direct and abdominal with reference heart beats annotations, 2020, http://dx.doi.org/10.6084/M9.FIGSHARE.C.4740794.V1.

[91] A.L. Goldberger, L.A. Amaral, L. Glass, J.M. Hausdorff, P.C. Ivanov, R.G. Mark, J.E. Mietus, G.B. Moody, C.-K. Peng, H.E. Stanley, PhysioBank, PhysioToolkit, and PhysioNet: components of a new research resource for complex physiologic signals, Circulation 101 (23) (2000) http://dx.doi.org/10.1161/01.CIR.101.23.e215.

[92] V. Gupta, M. Mittal, V. Mittal, A.K. Sharma, N.K. Saxena, A novel feature extraction-based ECG signal analysis, J. Inst. Eng. (India): Ser. B (2021) http://dx.doi.org/10.1007/s40031-021-00591-9.

[93] V. Gupta, M. Mittal, V. Mittal, Performance evaluation of various pre-processing techniques for r-peak detection in ECG signal, IETE J. Res. (2020) 1–16, http://dx.doi.org/10.1080/03772063.2020.1756473.

[94] J. Martin Bland, D. Altman, Statistical methods for assessing agreement between two methods of clinical measurement, Lancet 327 (8476) (1986) 307–310, http://dx.doi.org/10.1016/S0140-6736(86)90837-8.

[95] K. Lee, B. Lee, Sequential total variation denoising for the extraction of fetal ECG from single-channel maternal abdominal ECG, Sensors 16 (7) (2016) 1020, http://dx.doi.org/10.3390/s16071020.

[96] F. Andreotti, J. Behar, S. Zaunseder, J. Oster, G.D. Clifford, An open-source framework for stress-testing non-invasive foetal ECG extraction algorithms, Physiol. Meas. 37 (5) (2016) 627–648, http://dx.doi.org/10.1088/0967-3334/37/5/627.

[97] D. Gurve, S. Krishnan, Separation of fetal-ECG from single-channel abdominal ecg using activation scaled non-negative matrix factorization, IEEE J. Biomed. Health Inf. 24 (3) (2020) 669–680, http://dx.doi.org/10.1109/JBHI.2019.2920356.

[98] R. Sameni, C. Jutten, M. Shamsollahi, Multichannel electrocardiogram decomposition using periodic component analysis, IEEE Trans. Biomed. Eng. 55 (8) (2008) 1935–1940, http://dx.doi.org/10.1109/TBME.2008.919714.

[99] B. De Moor, P. De Gersem, B. De Schutter, W. Favoreel, DAISY: A database for identification of systems, J. A 38 (1997) 4–5.

[100] E. Castillo, D.P. Morales, A. García, L. Parrilla, V.U. Ruiz, J.A. Álvarez-Bermejo, A clustering-based method for single-channel fetal heart rate monitoring, PLoS One 13 (6) (2018) e0199308, http://dx.doi.org/10.1371/journal.pone.0199308.

[101] M. Ayat, K. Assaleh, H. Al-Nashash, Extracting fetal ECG from a single maternal abdominal record, in: 2015 IEEE 8th GCC Conference & Exhibition, IEEE, Muscat, Oman, 2015, pp. 1–4, http://dx.doi.org/10.1109/IEEEGCC.2015.7060027.

[102] Y. Zhang, S. Yu, Single-lead noninvasive fetal ECG extraction by means of combining clustering and principal components analysis, Med. Biol. Eng. Comput. 58 (2) (2020) 419–432, http://dx.doi.org/10.1007/s11517-019-02087-7.

[103] G. Da Poian, R. Bernardini, R. Rinaldo, Separation and analysis of fetal-ECG signals from compressed sensed abdominal ECG recordings, IEEE Trans. Biomed. Eng. 63 (6) (2016) 1269–1279, http://dx.doi.org/10.1109/TBME.2015.2493726.

[104] D. Panigrahy, P. Sahu, Extraction of fetal ECG signal by an improved method using extended Kalman smoother framework from single channel abdominal ECG signal, Australas. Phys. Eng. Sci. Med. 40 (1) (2017) 191–207, http://dx.doi.org/10.1007/s13246-017-0527-5.

[105] J. Sandall, R.M. Tribe, L. Avery, G. Mola, G.H. Visser, C.S. Homer, D. Gibbons, N.M. Kelly, H.P. Kennedy, H. Kidanto, P. Taylor, M. Temmerman, Short-term and long-term effects of caesarean section on the health of women and children, Lancet 392 (10155) (2018) 1349–1357, http://dx.doi.org/10.1016/S0140-6736(18)31930-5.

[106] E. Orovou, M. Dagla, G. Iatrakis, A. Lykeridou, C. Tzavara, E. Antoniou, Correlation between kind of cesarean section and posttraumatic stress disorder in greek women, Int. J. Environ. Res. Public Health 17 (5) (2020) 1592, http://dx.doi.org/10.3390/ijerph17051592.

[107] S. Petrou, J. Henderson, C. Glazener, Economic aspects of caesarean section and alternative modes of delivery, Best Pract. Res. Clin. Obstet. Gynaecol. 15 (1) (2001) 145–163, http://dx.doi.org/10.1053/beog.2000.0154.

[108] D.M. Okada, A.W. Chow, V.T. Bruce, Neonatal scalp abscess and fetal monitoring: factors associated with infection, Am. J. Obstet. Gynecol. 129 (2) (1977) 185–189, http://dx.doi.org/10.1016/0002-9378(77)90742-6.

[109] A.C. Mugdha, F.S. Rawnaque, M.U. Ahmed, A study of recursive least squares (RLS) adaptive filter algorithm in noise removal from ECG signals, in: 2015 International Conference on Informatics, Electronics & Vision (ICIEV), IEEE, Fukuoka, Japan, 2015, pp. 1–6, http://dx.doi.org/10.1109/ICIEV.2015.7333998.

[110] B. Sharma, R.J. Suji, ECG denoising using weiner filter and adaptive least mean square algorithm, in: 2016 IEEE International Conference on Recent Trends in Electronics, Information & Communication Technology (RTEICT), IEEE, Bangalore, India, 2016, pp. 53–57, http://dx.doi.org/10.1109/RTEICT.2016.7807781.

[111] D. Graupe, D. Veselinovic, Blind adaptive filtering of speech from noise of unknown spectrum using a virtual feedback configuration, IEEE Trans. Speech Audio Process. 8 (2) (2000) 146–158, http://dx.doi.org/10.1109/89.824699.

[112] K.-C. Yen, Y. Zhao, Adaptive co-channel speech separation and recognition, IEEE Trans. Speech Audio Process. 7 (2) (1999) 138–151, http://dx.doi.org/10.1109/89.748119.

[113] B. Widrow, J. Glover, J. McCool, J. Kaunitz, C. Williams, R. Hearn, J. Zeidler, J. Eugene Dong, R. Goodlin, Adaptive noise cancelling: principles and applications, Proc. IEEE 63 (12) (1975) 1692–1716, http://dx.doi.org/10.1109/PROC.1975.10036.

[114] V. Gupta, M. Mittal, A novel method of cardiac arrhythmia detection in electrocardiogram signal, Int. J. Med. Eng. Inform. 12 (5) (2020) 489, http://dx.doi.org/10.1504/IJMEI.2020.109943.

[115] A. Giorgio, C. Guaragnella, D.A. Giliberti, Improving ECG signal denoising using wavelet transform for the prediction of malignant arrhythmias, Int. J. Med. Eng. Inform. 12 (2) (2020) 135, http://dx.doi.org/10.1504/IJMEI.2020.106898.